

ANALYSIS OF ASPECTS
OF THE GEO 600 STYLE
TRIPLE AND QUADRUPLE SUSPENSION
SYSTEMS FOR ADVANCED LIGO

California Institute of Technology SURF Program 2002
Final Report
LIGO-E020811-00-D

Mentor: Dr. Calum I. Torrie
LIGO Caltech
ctorrie@ligo.caltech.edu

Daniel Mason
Rensselaer Polytechnic Institute
Caltech UID: 0001466946

Contact: masond2@rpi.edu
518-272-9539

Table of Contents

1.	<i>Introduction to LIGO and Suspensions</i>	3
2.	<i>Experiments</i>	4
2.1	ALGOR Blade Deflection Modeling	5
2.2	Wire Testing	7
2.2.1	Breaking Stress	7
2.2.2	Young's Modulus	9
2.3	Upper Mass Bending Model	10
2.3.1	Force Method	11
2.3.2	Force and Moment Method	13
2.4	Cold-Welding Test	18
3.	<i>Conclusions</i>	21
4.	<i>References</i>	22

Appendix A: Wire-Breaking data

Appendix B: Young's Modulus data

Appendix C: Upper-mass Bending Model Results

Appendix D: Cold-welding data

Appendix E: Drawings

1. An Introduction to LIGO

The Laser Interferometer Gravitational Wave Observatory (LIGO) is an international collaboration of physicists and engineers working together in the search for gravitational waves. Gravitational waves are ripples in space-time emitted by super-dense objects in space, such as black holes and binary stars. They have been predicted by Einstein and proved indirectly, but the goal is that the LIGO project, along with its counterparts around the world, will finally prove their existence without question [1]. LIGO currently has facilities on two sites in Hanford, Washington (see Figure 1.1), and Livingston, Louisiana, with which gravitational waves will be detected. Potential changes and upgrades to the current facilities are conceived, designed, and tested at the California Institute of Technology (Caltech), the Massachusetts Institute of Technology (MIT), and GEO 600 German-British Collaboration.



Figure 1.1: LIGO Hanford Site [2]

LIGO will use an approach known as interferometry to detect gravitational waves. Light from a laser beam enters the two arms of the interferometer at right angles to each other. The setup will be able to

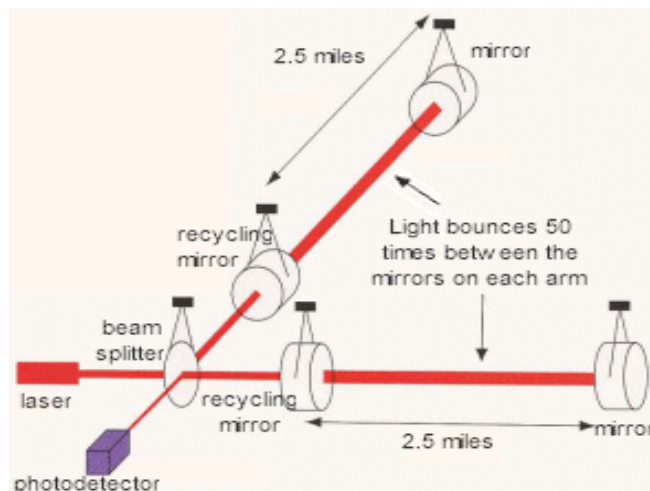


Figure 1.2: LIGO Interferometer [2]

measure changes in the length of the arms due to gravitational waves, as shown in Figure 1.2. If there is any change in the length of the arm, a change in the light intensity will be detected by a photodetector.

However, the expected change is so small that it will be nearly impossible to detect without filtering out noise from photon, thermal, and seismic sources. Advanced

LIGO will incorporate new designs to reduce each one of these to acceptable values. One way the seismic system provides isolation is by mounting the optics on triple and quadruple pendulums, developed for LIGO by Dr. Calum Torrie, et al. The pendulums will complement the active noise damping by hydraulic actuators outside the chambers. For a pendulum, a suspended mass will oscillate with very high displacement if excited at its resonant frequency, but above this frequency the displacement/transmissibility falls off as $1/f^2$ per stage [3]. This means at relatively high frequencies there is very little movement in a suspended mass. Multiple stages provide even greater performance. Voice coil actuators mounted on the upper stages supply additional damping at resonant frequencies.

In the summer of 2001 Dr. Torrie & colleagues of the University of Glasgow delivered and installed the first generation quadruple-pendulum prototype to MIT. The design, shown in Figure 1.3, is based on the triple pendulum used in the GEO 600 [3]. Work on the second-generation prototype that will include optimizations of the initial prototype has been ongoing. It is on refining and investigating different aspects of this pendulum that has constituted most of the research this summer.



Figure 1.3: Quadruple Pendulum Prototype

2. The Experiments

A number of experiments were conducted over the course of the summer to study various physical behaviors of the pendulum design that will be important in the design and construction of the next set of prototypes. Several of these experiments were conducted in conjunction with John Veitch, an undergraduate at the University of Glasgow, and fellow SURF student.

Included in these experiments was a finite-element analysis of blade deflections, extensive testing of wire for properties of Young's modulus and breaking stress using different clamping techniques, modeling the bending of a pendulum upper stage, and an investigation into the phenomenon of galling/cold-welding in both stainless steel and aluminum.

2.1 ALGOR Blade Deflection Modeling



Figure 2.1 Cantilever blade

Upper stages of the pendulum are fitted with cantilever blades to enhance the vertical isolation [3]. The thicker end is mounted with clamps to the upper mass, while wire is clamped to the thinner end to suspend the stages below. It is important that when the load is applied the blades lie flat, as the position of the overall system and the ability to control individual parameters are dependant on the blades. Experiments performed in the laboratory obtained an actual value for the mass necessary to flatten.

ALGOR, Inc. [4] finite element analysis software was then used to model the application of load and flattening of the blade. The goal of the project was to find the correct method for obtaining a value most realistic to the one measured. The problem was in getting the program to come even close to the actual deflection value when a load is applied with the intent to flatten the blade. A number of different procedures were attempted, but to no avail. The ALGOR help line was contacted on a regular basis did their best, but in the end was unable to help the situation.

The underlying challenge was in applying a force at the tip of the blade that would always remain perpendicular to the surface. Different approaches ranged from changing the geometry to different loading conditions and analyses. One approach involved creating a flat surface at the end of the blade and applying a distributed load. This approximation is quite different from reality, however, and an adequate deflection was not achieved. Other attempts included applying a load parallel to the surface at the tip of the blade and performing different types of analyses. Of particular note, a mistake in the programming code was discovered and reported to the ALGOR technical support, whom promised to bring the issue to the attention of the programmers. This mistake was found when identical loading and constraint conditions were applied to the blade in both the Linear Static Stress and Mechanical Event Simulator analysis types but each type returned a very different answer. In the end, a successful procedure was finally discovered. It is important to note that to proceed and find success, the Solidworks [6] model of the blade must be altered so that there is a flat section on the top of the blade at the wire-clamp tip. The steps are outlined on the following page.

Directions for analyzing blade deflection in ALGOR:

1. Import blade model from Solidworks [6] and mesh to size 40. Do not automatically solid mesh.
2. Open up the Solid Mesh Engine by clicking Mesh / Solid Mesh Generation
3. In the Solid Mesh Engine window click on “Options” followed by the “General Controls” tab and check the box marked “Use Thin Cross-Section Scheme.”
4. Proceed by generating solid mesh
5. Click on Tools / FEA Object Editor
6. Specify Material
7. Fix both top and bottom surfaces at the blade clamp (thicker) end
8. To the flat surface at the wire clamp end, apply a “Surface Load” in the form of a “Uniform Pressure” of 537502 N/m^2 (equal to the force required of 78.4 N / area of end of $1.46\text{E-}4 \text{ m}^2$)
9. Perform analysis

As shown in figure 2.2, by following this procedure ALGOR returns a value of 95.6 mm, as compared to the actual measured value of 103 mm. This method considers the load of the wires as a pressure, which allows it to be perpendicular to the surface throughout the bending process.

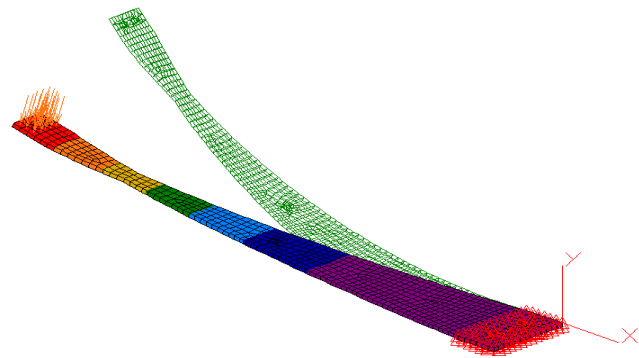


Figure 2.2 Algor model of deflecting blade

However, it is still an approximation since the pressure is distributed over a fairly large area. Due to time constraints additional adjustments to the procedure could not be used in obtaining a closer deflection value. Future work is recommended in reducing the flat area at the tip of the blade to a very small amount and essentially creating a load at a single point or distributed over a line. Concentrating the pressure at the extreme tip of the blade will produce a larger, as well as being closer to actual, deflection. Also, the first prototype design included wire clamps which extended an additional distance from the end of the blade, creating a larger moment and deflecting the blade more than expected. It is recommended that future work include the blade and wire clamp assembly for the most accurate results.

2.2 Wire Tests

Extensive wire testing was done in order to compare the properties of twelve wires of different diameters from three different manufacturers. The focus of the investigation was on Young's modulus and breaking stress for each wire. The breaking stresses were measured using three different clamping arrangements, as shown in Figures 2.4a-c on the following page.

Because the wires are an integral part of the suspensions, choosing the right type is very important to avoid failure under the high loads that will be applied to it. The pendulums are designed such that the wires will have a factor of safety of three, that is, the maximum stress a wire will be subject to will not exceed one third of its breaking stress. Knowing the accurate Young's modulus of a wire is also important when calculating the modes of the pendulum. Each wire came with manufacturer's specifications. However, due to the fact that the wire will be clamped and loaded differently in LIGO (as in Figure 2.5) than they were when tested at the manufacturer's laboratories, both the breaking stress and Young's modulus will be investigated.

2.2.1 Breaking Stress

The experimental setup for measurement of the breaking stress, as shown in Figure 2.3, consisted of a length of wire mounted between two clamps with a hook (or platform for larger thicknesses) suspended below. The entire apparatus was then hung from a shop crane surrounded by a clear plastic tube for safety. For each length of wire tested, masses were slowly applied to the hook/platform until the wire failed. Care was taken to apply only very small mass increments as the expected breaking value (calculated using manufacturer-supplied numbers) was approached. Each thickness of wire was tested several times to ensure that a clear value for breaking stress was obtained.

Three different types of clamps were used for comparison. The first, known as the "initial clamp" was treated as a worst-case scenario. The two pieces of the clamp were rarely correctly aligned and the insides were scarred from repeated use. An upgrade from that was the

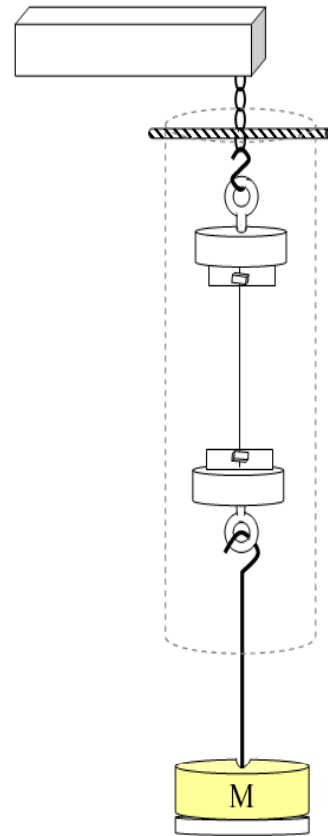


Figure 2.3 Breaking stress setup

“machined clamp,” which had the hole separation tolerance and hole size reduced for a tighter, more consistent fit. Another addition from the initial clamp was a groove of given depth that is wire-specific and fly cut surfaces for even clamping. These are the same types of clamps that are currently used in GEO 600 and LIGO I. The “round clamp” is clamped like the initial clamp but wrapped around a cylinder to provide an alternate form of clamping.

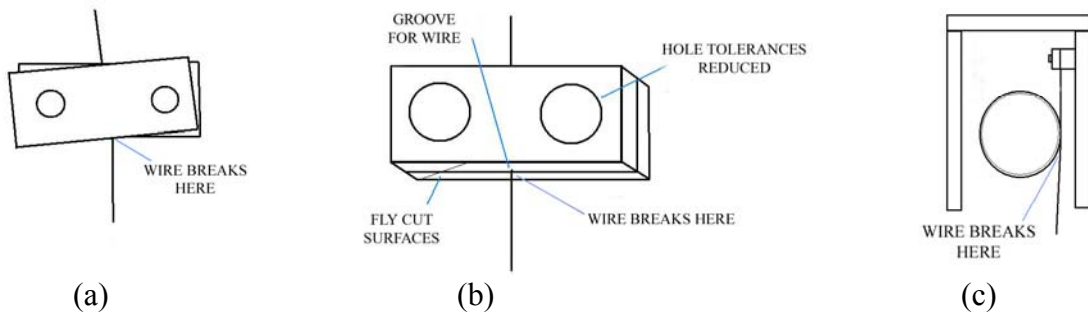


Figure 2.4 Wire clamps used in experiment: (a) initial clamp, (b) machined clamp, (c) round clamp

The experiment yielded many results for analysis. The most important data was in the comparison of relative wire strengths in each clamp. As expected, the initial clamp yielded results which were significantly below the expected strength value for a wire in tension. The machined clamp showed significant improvement over the initial clamp, on the order of 15% higher breaking stress for those wires tested. The round clamp, however, had an increase of more than twice the strength over the initial clamp. It should be noted that in the initial and machined clamps the wires consistently broke at the clamp (due to “pinching” of the wire), whereas wires in the round clamp would consistently break where the wire leaves the cylinder. Complete results can be viewed in Appendix A, and a complete analysis of all wire diameters, manufacturers, and clamping techniques can be viewed in the report submitted by John Veitch [5].

A look at the data suggests that wire clamps would be better suited to handle large loads if exhibiting some of the qualities of the round clamp, or more specifically, if a round surface was incorporated for the wire to follow as it leaves the wire clamp. The suggestion for additional experimentation is

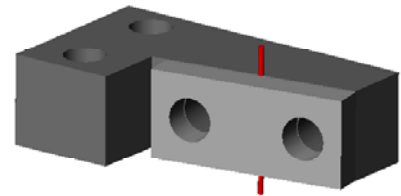


Figure 2.5 MIT Prototype wire clamp

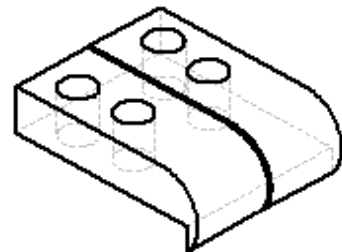


Figure 2.6 Rounded wire clamp

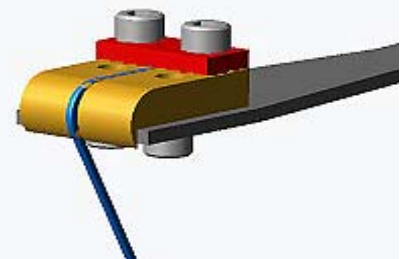


Figure 2.7 Rounded blade assembly

a rounded clamp adapted for use on the blades, or what turns out to be a hybrid of the round and machined clamp, as shown in Figures 2.6 and 2.7. The wire is clamped in a traditional way, but the hope is that a lesser degree of weakening at the clamp will occur. The most important aspect of the design is the rounded end, allowing the wire to smoothly leave the clamp and take advantage of the higher breaking stresses of the round clamp. The rounded edge extends so that in nearly all orientations in which the clamp will be used the wire will not be sheared by the edge created at the end of the round portion. This design is now being tested in the lab.

2.2.2 Young's Modulus

The Young's modulus (the modulus of elasticity) of the wire was also measured and compared to company specifications using two different setups, one by measuring the vertical "bounce" of the wire and the other by the frequency of rotation. In the vertical approach of Figure 2.8, a length of wire approximately seven meters long was suspended by the ceiling of the lab using a crane (Figure 2.8 and 2.9). A mass was then applied and the setup was excited to bounce at its natural frequency. The frequency was determined by counting the number of bounces in a given amount of time as in Figure 2.10 (in later steps it was measured more accurately with an accelerometer) and Young's modulus was calculated by:



Figure 2.8
Vertical setup

$$E = \frac{4\pi f^2 m}{r^2} \quad (2.1)$$

where f is the frequency of oscillation, m is mass suspended by the wire, and r is the radius of the wire.



Figure 2.9 Wire mounting to crane



Figure 2.10 Veitch demonstrates proper frequency measuring technique

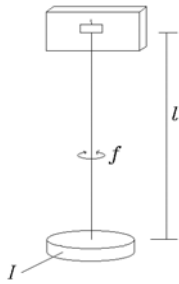


Figure 2.11
Rotational setup

To calculate Young's modulus by the rotation of the wire, a sample wire of much shorter length (approximately 15 cm) was mounted between two clamps and held against the edge of a table to keep it steady. The bottom clamp was then twisted at a small angle and the frequency was measured by the number of oscillations in a given time, as shown in Figure 2.11. Young's modulus can then be calculated by:

$$E = \frac{\pi I f^2 l (1 + \sigma)}{r^2} \quad (2.2)$$

where f is the rotational frequency, I is the moment of inertia of the bottom clamp, l is the length of the wire, σ is Poisson's ratio (taken to be 0.29 [7]), and r is the radius of the wire.

The results obtained in these experiments were generally similar, with the highest percent difference between the two approaches at 18% but a majority below 10%. Most were around the same value as well (~180-200 GPa) with the exception of the .45mm Knight wire, which also gave some unexpected results in the breaking stress tests. Appendix B lists the complete set of data and calculations and Veitch's Paper gives more detailed analysis of the data.

2.3 Upper Mass Bending Model

The first-generation quadruple pendulum that was constructed in 2001 at MIT will require several design changes before the construction of the next prototype. One of these was in upper masses, located as shown in Figure 2.12 and similar to Figure 2.13b, which tended to bend due to the loading of the blades. The blades were bolted at opposite ends of the mass platform and extended across to the opposite side when loaded and flattened. This loading at the very ends of the mass caused the ends to bend up, as shown in Figure

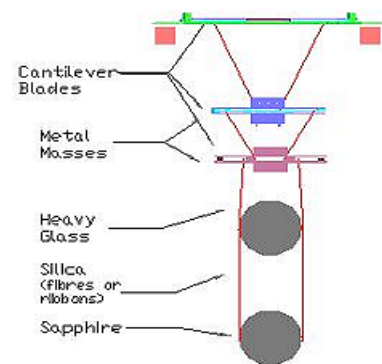


Figure 2.12 Quadruple pendulum

2.13a. The bending will change both the spacing between the stages and the overall length of the pendulum, both of which are important dimensions for the optic to be in the correct plane and for optimal coupling of stages.

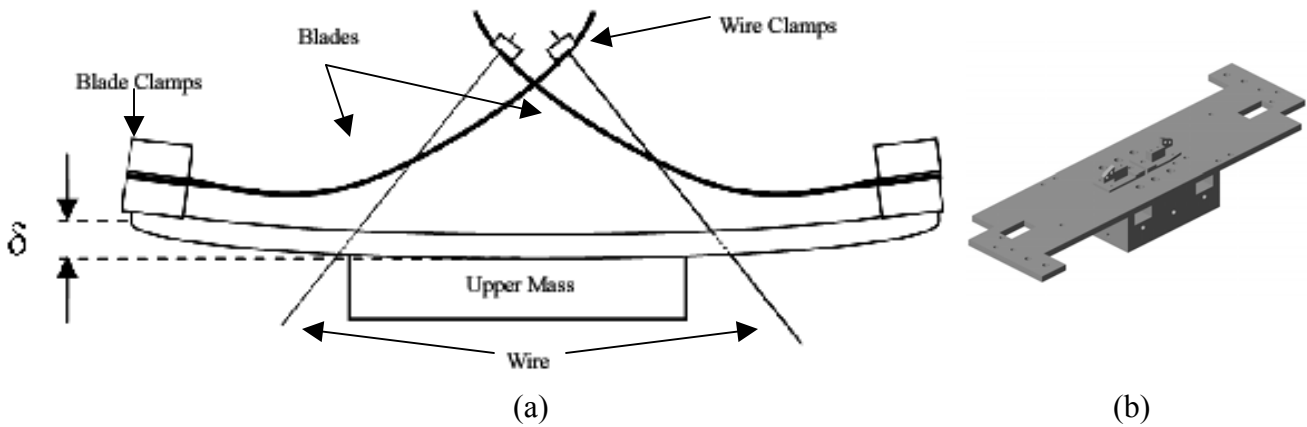


Figure 2.13 Upper Mass: (a) loaded, side-on view, bending exaggerated, (b) solid model

The in-process solution at MIT was the addition of stiffening bars to the masses, but in the future the solution will be incorporated in the design of the upper masses. To aid in this design is the following derivation of formulae, which will predict the amount of deflection under given parameters. The deflection of the upper mass was modeled by approximating half of the upper mass as a cantilever beam. This was done because modeling the mass as pure bending (which at first glance seems the most fitting) assumes a constant radius of curvature, which was not seen due to the varying cross section (and moment of inertia). It was determined that the characteristic bending behavior of a transversely-loaded cantilever beam was the most accurate model of the actual upper mass.

Two approaches will be presented: one in which the formula is derived through forces and one in which forces and moments are used. It has been shown that these give nearly equal results.

2.3.1 Approach #1: Force Method

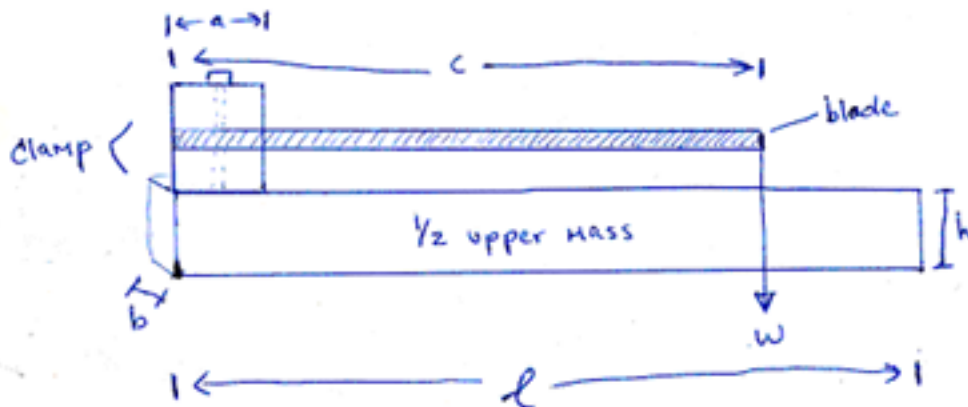


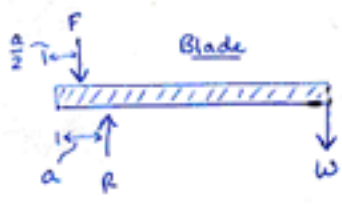
Figure 2.14

Figure 2.14 consists of one half of the upper mass assembly. Variables are assigned to the following quantities:

- a is the width of the clamps
- b is the width of the upper mass
- c is the length of the blade
- h is the thickness of the upper mass
- l is half the length of the upper mass (or the entire length of the bar used as a model).

The first step is to balance the forces in the blade so that reactions in the clamp may be found.

I. Force / Moment Analysis



$$\sum F = R - F - W = 0 \quad (2.3)$$

$$\sum M_F = \frac{a}{2}R - (c - \frac{a}{2})W = 0 \quad (2.4)$$

$$\frac{a}{2}R = (c - \frac{a}{2})W \quad (2.5)$$

$$R = \frac{2W(c - \frac{a}{2})}{a} \quad (2.6)$$

$$R = \frac{W(2c - a)}{a} \quad (2.7)$$

$$F = \frac{W(2c - a)}{a} - W \quad (2.8)$$

*R placed at corner of clamp
F at bolts*

Figure 2.15

Transferring these forces to the upper mass arrives at the following cantilever set up:

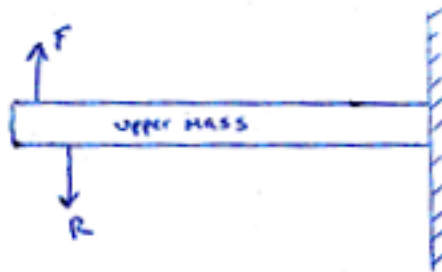


Figure 2.16

To solve the deflection in the upper mass, the deflections caused by each of the forces will be superimposed and a resultant deflection found. The next step is to translate the reference formula to the variables being used in the model.

II. Translation of Formula

Reference [7]:

$$f = \frac{wL^2}{6EI} (2L + 3b)$$



Converted:

reference	$\frac{F}{L}$	$\frac{R}{L-a}$	(2.9)
L	$L - \frac{a}{2}$	$L - a$	
b	$a/2$	a	
$2L + 3b$	$2L + \frac{a}{2}$	$2L + a$	

Figure 2.17

III. Substitution

Substituting the values into the equation gives the following equation for the deflection of the mass (where a positive deflection is the mass bending up):

$$f = \frac{F(L - \frac{a}{2})^2}{6EI} (2L - \frac{a}{2}) - \frac{R(L-a)^2}{6EI} (2L + a) \quad (2.10)$$

$$\text{where } F = \frac{w(2L-a)}{a} - w \quad (2.8)$$

$$R = \frac{w(2L-a)}{a} \quad (2.7)$$

$E = \text{Modulus of Elasticity}$

$$I = \frac{1}{12} b h^3 \quad (2.11)$$

2.3.2 Approach #2: Force and Moment Method

Conceived with the help of Phil Willems, the following method uses one reaction force and a moment instead of using only forces. The reaction force is equal to the weight applied at the end of the blade (or, in terms of the previous approach, it is the resultant of reaction forces F and R). The moment (couple) is also due to the applied load, and has a magnitude of the weight times the length of the blade. This results in a cantilever beam under this loading with deflection equations [7],[8] shown on the following page.

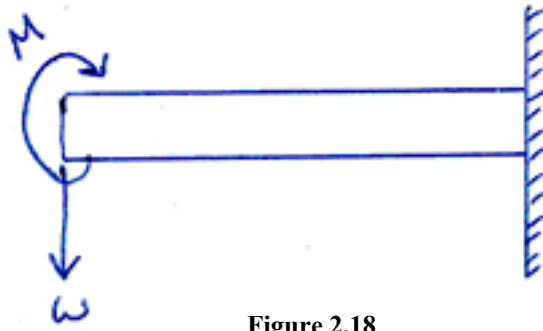


Figure 2.18

$$\text{Deflection due to } w: \delta = -\frac{wl^3}{3EI} \quad (2.12)$$

$$\text{Deflection due to } M: \delta = \frac{wcl^2}{2EI} \quad (2.13)$$

Combining these deflections the following formula is obtained:

$$\delta = \frac{wcl^2}{2EI} - \frac{wl^3}{3EI} \quad (2.14)$$

One interesting result of this approach is that it can be predicted whether a beam will curve up or down depending on the lengths of the blade and mass. The mass will curve up when:

$$\frac{c}{2} > \frac{l}{3} \quad (2.15)$$

To test these equations, an experiment was devised that would measure the deflection of an aluminum bar with a loaded blade attached, as shown in Figures 2.19a-b to the right.

The aluminum bar representing the upper mass was approximately 60 cm long to allow for significant deflection, which made measurements easier and the calculations more accurate. It was found that when using shorter bars the numbers were so small that although the absolute

error was not particularly large, the percent error was very significant. The mass is fastened to the optical table with a

spacer in between. A hole was located along the mass in such a location that it allowed for the wire between the blade and masses to pass through the mass. A height gauge was used to measure the difference between the loaded and unloaded heights by zeroing at the unloaded position, applying masses, and remeasuring.

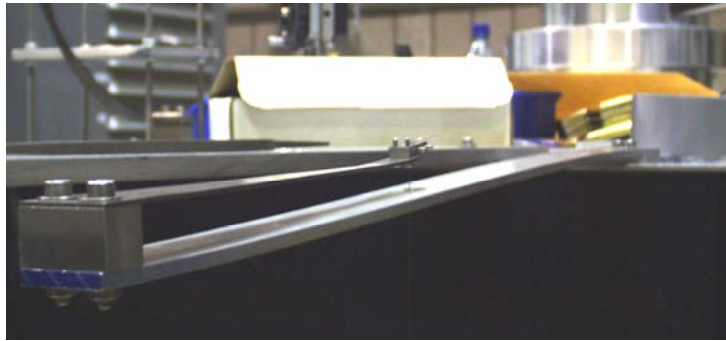
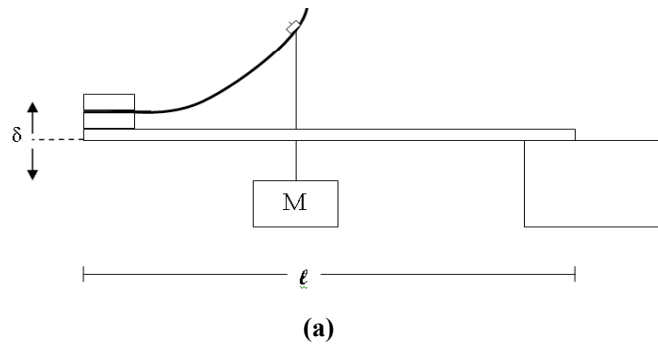


Figure 2.19 Experimental setup: (a) schematic, (b) actual

Deflection Calculator		
Inputs		
a	width of clamps	0.02
b	width of upper mass	0.038
l	length of upper mass	0.597
h	thickness of upper mass	0.00634
c	length of blade	0.26
	width of blade	0.025
	thickness of blade	0.0023
d	mass overhang	0
m	mass applied	7.88
Calculations		
w	Force Applied	77.3028
R	Reaction Force (Down Push)	-1932.57
F	Reaction (Push Up)	1855.2672
I	Moment of Inertia	8.07E-10
E	Modulus of Elasticity	6.90E+10
Models		
Force Model, eq. 2.10		
	Deflection Down	-2222.400
	Deflection Up	2188.962
	Overall deflection (Eq. 1)	-33.44
Force/Moment Model, eq. 2.14		
	Force	-98.464
	Moment	64.323
	Overall Deflection (Eq. 2)	-34.14
	Average:	-33.79

Figure 2.20 Deflection calculator screenshot

Results from the equations 2.10 and 2.14 can be entered into an Excel worksheet where variables can be easily changed to predict the optimum design for an upper mass [9]. In the meantime, the calculator can be used to test the theory behind the equations by comparing the calculated and measured results. Figure 2.20 to the left is an excerpt from the measurement of the ¼” aluminum bar.

Values for each of the variables can be entered into the “Inputs” section of the calculator. The units are in meters, for ease of calculation. Below this, in the “Calculations” section, the values for the forces involved in the calculation were found. The moment of inertia was calculated for a rectangular cross-section using the equation:

$$I = \frac{1}{12}bh^3 \quad (2.15)$$

(where b is width of bar and h is thickness)

Young’s modulus is a material property and will remain constant with the material.

In the “Models” section both deflection models were calculated using Equation 1 and 2. They are first expressed in their up/down components and then their resultant, expressed as the overall deflection. Deflection values for the Force Model were calculated using forces F and R (resulting in up and down deflection, respectively). Below that is the calculation of the Force/Moment Model, showing the deflections due to the force, moment, and the overall deflection. The average deflection is the mean of the deflections in both models, and was used for comparison against measured data.

Tables in Appendix C show some of the results obtained. The model fits very closely with each set of experimental results. The percent difference between the calculated and measured value never exceeded 8% and were well below that level at most points. Positive results were also seen when comparing the bending of the actual upper mass at MIT with calculated numbers. The measured deflection of the mass (which was made of Aluminum and 8mm thick) was approximately 10mm, as compared with a calculated value of 8.1mm.

For future prototypes, it is intended to design the upper mass such that the flat platform piece alone will be able to withstand the bending forces exerted by the loaded blades. This way, all additional structural support offered by the rest of the upper-mass assembly is added in as a factor of safety. Acceptable bending amounts will be considered to be under 1mm. The final design for the upper mass will be dictated by the actual suspension configuration decided upon by Norma Robertson. Provisional plans imply the Advanced LIGO test mass suspensions will have a thickness, for aluminum, of between 18mm for the lightest configuration and 21mm for the heaviest. An upper mass made of stainless steel should be between 13mm and 15mm. The lightest and heaviest configurations are, from top to bottom: 22, 22, 22, 40 kg and 24, 24, 48, 40 kg respectively [10],[12].

2.4 Cold-Welding Test

Cold-welding, also known as galling or freezing, is the fusing of a moving part through excessive pressure, temperature, or friction. It occurs most commonly between two materials of very similar hardness because neither material will easily deform in the event of defects



Figure 2.21 Frozen steel screw in a stainless steel optical table

in the threads. It is even more frequent in the absence of lubricants and under very

clean conditions similar to those found in LIGO. A cold-welded screw in a LIGO vacuum chamber may cost the project thousands of dollars in replacement parts and weeks in delays, so every effort must be made to avoid such instances. This experiment is being carried out due to differing suggestions among the area machine shops as to what hole size and tolerance should be used to avoid cold-welding.

	Tap Drill Size	Range
4-40 UNC-2B	0.0938	.0958 - .0991
4-40 UNC-1B	0.0960	.0958 - .1012
4-40 .003 Oversize	0.0980	.0988 - .1042
1/4-20 UNC-2B	0.2055	.2175 - .2224
1/4-20 UNC-1B	0.2090	.2175 - .2248
1/4-20 .005 Oversize	0.2130	.2225 - .2298

Table 2.1 Threaded hole tap drill size and pitch diameter range [8]

In this experiment several different variables will be measured. First, two sizes of fasteners were used, 4-40 and 1/4-20 socket head cap screws, the most common sizes used in suspensions. These screws were made of silver-plated stainless steel. Also, the base plate into which these screws were placed consisted of

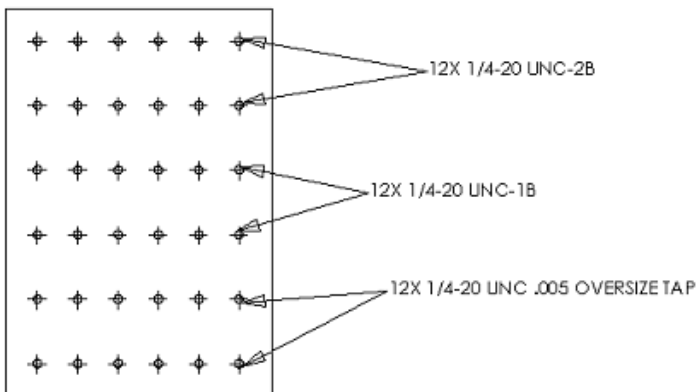


Figure 2.22 Base plate layout, 1/4-20 holes

either stainless steel or aluminum. Finally, the most important factor to be tested was the type of hole. Each base plate had holes of three different thread classes: UNC-2B, UNC-1B and oversize tap. The first two are standard thread classes (2B being the most

common) and the oversize hole was a custom-made tap. Detailed information for each hole is shown in Table 2.1.

Rows of six holes were assigned to each combination of sizes and materials. As shown in Figure 2.22, a given base plate has two rows of each type of hole. The top row was designated as being for the stainless screws, the bottom row for the silver-plated screws.

All parts to be used were cleaned and baked to LIGO specifications [11]. This included ultrasonic cleaning in Liquinox, rinsing in distilled water, ultrasonic cleaning again in a methanol bath, and then baking in vacuum (at 200 8C for aluminum, 1208C for stainless steel) for 48 hours. The experiment was carried out under LIGO clean-room conditions with gloves and facemask to prevent the transfer of saliva and body oils, which are potential lubricants.

The procedure of the experiment was fairly simple. Each screw was torqued to a given value using a torque wrench (as shown in Figure 2.23) and then unscrewed by hand using an Allen wrench. Upon unscrewing, the relative ease at which the screw was undone was determined subjectively by the following scale:



Figure 2.23 Torquing of Screws

1. Very easy to unscrew (can be done with one finger)
2. Small amount of friction
3. Very hard to unscrew
4. Frozen in place

The 4-40 screws were torqued at 5, 8, 12, 16, and 20 in-lbs (recommended torque is 5 in-lbs) and the ¼-20 screws were torqued at 12, 20, 40, 60, and 80 in-lbs (recommended torque is 65 in-lbs).

The results obtained were compelling. There was a very high occurrence of freezing with stainless screws in stainless plates and silver-plated screws in aluminum plates in the UNC-2B and UNC-1B holes. These were the expected circumstances (similar hardness, tight hole tolerance) in which cold-welding would occur and it did so consistently and at low torque. No cold-welding occurred in the holes of differing hardnesses: the stainless steel screws in aluminum plates and silver-plated screws in stainless

plates. The oversized holes performed much better than expected, and in all combinations of materials only one screw became frozen. Full results can be found in Appendix D.

One very interesting result to note is that in the 4-40, silver-plated screws in stainless plates, every screw sheared off around 18-20 in lbs. This occurred in each type of threaded hole, and without warning; in the UNC-1B and oversize holes, almost every screw was very easy to unscrew until it broke off. In other instances of fastener breaking that was seen in the experiment, it occurred only after the screw had frozen and



Figure 2.24 Screws deformed after freezing

additional torque was added. Another observation was that the same type of screw was torqued to 20 in-lbs in the aluminum plates and no shearing was observed. It is recommended that additional research and experimentation be done to investigate this strange result.

Based on these results it is recommended that stainless-steel fasteners continue to be used in aluminum components and silver-plated fasteners in stainless-steel. The use of oversize taps is also recommended, though the additional cost may not justify their use. In lieu of oversize taps though, the use of UNC-1B taps showed significant improvement over UNC-2B, and in many cases their performance was equal to that of the oversize taps. As far as torque recommendations go, in most cases of optimal material combinations the fasteners were not brought all the way to a state of galling due to the limitations of the torque wrenches used. So, the recommended torques will be determined based on the highest applied torque in which (nearly) all of the fasteners were at level 2 (small amount of friction) in the UNC-2B tap size. In the case of 4-40 silver-plated fasteners in stainless plates, the suspensions standard factor of safety

	Recommended Max Torque, in-lbs.	
	4-40 Bolts	1/4-20 Bolts
Silver plated bolts in Stainless	6	40
Stainless bolts in Aluminum	20	60

of three will be used. The recommended torques are shown in Table 2.2.

Table 2.2 Recommended Torques

3. Conclusions

Much work was done over the course of the ten week program which should contribute significantly to the progress of the second generation of pendulum design in LIGO. The exact process for modeling blade deflection was determined in ALGOR for use in future blade design to ensure that the blades lie flat under loading to keep the system in the desired position. The method described is for the blade only, so actual blade deflection analyses with ALGOR should be done with the wire clamp attached for greater accuracy.

Many wires of differing diameters, materials, and manufacturers were tested for their strength under several clamping conditions to ensure that the wire of proper strength is chosen for each stage. This testing also led to the development of a new blade clamp which will reduce the chances of wire failure. Time constraints limited the sample sizes of the wires tested, and larger sample sizes will yield better average strength values. It was suggested that an alternate way of applying mass could be by the addition of sand, which would give much more accurate numbers of breaking stress. This allows for nearly infinitesimally smaller weight-addition steps. This method, however, requires large volumes of sand and a large, strong container to hold it in. There is also the potential for a large mess.

The same wires were also tested for their Young's moduli, which will also be an important value in predicting the dynamics of the pendulum. The frequency was measured by manually counting the number of oscillations in a period of time, which is inherently inaccurate (though the error is probably insignificant for the purposes of the experiment). It is recommended that any future frequency measurement be done with an accelerometer. Only a couple wires were done by this method, and it proved far superior in terms of accuracy and ease-of-use.

A mathematical model was created in order to predict the bending of the upper mass to once again ensure proper positioning of the stages. This model, in Excel format, was successful in predicting the deflection of long, thin beams and also in verifying the deflection seen in the prototype quadruple pendulum. Additional work may be recommended in testing the model with shorter, thicker experimental beams which are more similar to the actual upper mass. Also, additional means of stiffening the upper mass (which may be more efficient) should also be explored in addition to increasing the thickness. The upper mass could also be examined in ALGOR, as well.

Finally, the cold-welding tests were done to determine safest combination of materials and threading types for fasteners in clean conditions. It is highly recommended that additional work be conducted on the 4-40, silver-plated screws in a stainless plate. Such peculiar behavior may produce unexpected, if not disastrous results if the conditions are right.

The next generation of triple and quadruple pendulum suspensions are being developed now for delivery and testing at MIT in the latter part of 2003. Installation at the sites is planned for 2007.

4. References

- [1] LIGO: Catching the Gravitational Wave
- [2] About LIGO, http://www.ligo.caltech.edu/LIGO_web/about/
- [3] C. I. Torrie, PhD Thesis, University of Glasgow, 1999.
- [4] <http://www.algor.com/>
- [5] J. Veitch, Advanced LIGO Suspension Research, 2002.
- [6] <http://www.solidworks.com/>
- [7] E. Oberg and F.D. Jones, Machinery's Handbook, 19th edition.
- [8] Formulas for Stress and Strain, Shear, Moment and Deflection Formulas for Beams, *Reference number 9: Cantilever, end couple*
- [9] <http://www.ligo.caltech.edu/~ctorrie/>
- [10] N A Robertson, G Cagnoli, D R M Crooks, E Elliffe, J E Faller, P Fritschel, S Gosler, A Grant, A Heptonstall, J Hough, H Luck, R Mittleman, M Perreur-Lloyd, M V Plissi, S Rowan, D H Shoemaker, P H Sneddon, K A Strain, C I Torrie, H Ward and P Willems. *Class. Quantum Grav.* 19 No 15 (7 August 2002) 4043-4058
- [11] *Cleaning and Baking Procedures for Approved and Provisionally Approved Materials*, LIGO-E960022-07
- [12] Personal communication with Norma Robertson.

Appendix A: Wire-Breaking Data

Wire Type	0.2mm Elgiloy	0.2mm grooved clamp	0.2mm round clamp	0.2mm (kink)	0.22mm Malin	0.22 Malin round	0.30mm Malin	0.30 Malin round	0.30mm Malin grooved	0.30mm California
Breaking Mass (kg)	4.75	4.9	5.2	0.9	9.8	11	15.8	17.4	18	14.4
	4.85	5	5.2		9.75	11	15.4	17.4	17.8	14.8
	4.75	4.9	5.2		9.7	10.9	14.8	16.8		14.1
	4.45		5.2		9.9	11.02	14.8	17.45		
	4.6				9.5		15			
	4.85									
	4.85									
	4.8									
	4.75									
	4.45									
Average breaking mass	4.71	4.93	5.20	0.90	9.73	10.98	15.16	17.26	17.90	14.43
Mass inc hook	5.56	5.78	6.05	1.75	10.58	11.83	17.96	20.06	18.75	15.28
Standard Error	0.049	0.033	0.000		0.066	0.027	0.194	0.155	0.100	0.203
Diameter (mm)	0.2	0.2	0.2	0.2	0.22	0.22	0.3	0.3	0.3	0.3
Cross section (m ²)	3.14E-08	3.14E-08	3.14E-08	3.14E-08	3.80E-08	3.80E-08	7.07E-08	7.07E-08	7.07E-08	7.07E-08
Predicted Breaking mass	5.514	5.514	5.514	0.000	11.559	11.559	20.917	20.917	20.917	20.593
Breaking Stress (Pa)	1.73E+09	1.80E+09	1.89E+09	5.46E+08	2.73E+09	3.05E+09	2.49E+09	2.78E+09	2.60E+09	2.12E+09
Company's value	1.72E+09	1.72E+09	1.72E+09		2.98E+09	2.98E+09	2.90E+09	2.90E+09	2.90E+09	2.86E+09
Error in Breaking Stress	1.54E+07	1.04E+07	0.00E+00		1.71E+07	6.98E+06	2.69E+07	2.14E+07	1.39E+07	2.81E+07

Wire Type	0.34mm Elgiloy	0.34mm round	0.34 mm light kink	0.34 mm (kink)	0.35 Malin	.35 round	0.35 mm Califor	0.35 mm Californi	0.40mm Malin	0.40 mm round	0.45mm (Gla)	0.45mm round
Breaking Mass (kg)	18.35 16.4 17.4 17.7 17.95 17.4 13.4	18.6 18.3 18.3 18.2	14.4 14.3	2.5	17.6 18.8 18.5 19.9 17.9	22.5 22.7 22.3 22.3	17.2 16.8 19.2 19.2	25.2 24.7	25.4 25.4 24.6 24.9 25.7	31.8 31.4 30.4 31.1	31.3 28.8 31.8 23.4 23.4	33.3 30.8 32.9 34.7 31.9
Average breaking mass	16.94	18.35	14.35	2.50	18.54	22.45	18.10	24.95	25.20	31.18	27.74	32.72
Mass inc hook	19.74	21.15	17.15	3.35	19.39	23.30	18.95	25.80	26.05	32.03	30.54	35.52
Standard Error	0.633	0.087	0.050		0.401	0.096	0.640	0.250	0.197	0.295	1.843	0.658
Diameter (mm)	0.34	0.34	0.34	0.34	0.35	0.35	0.35	0.35	0.4	0.4	0.45	0.45
Cross section (m^2)	9.08E-08	9.08E-08	9.08E-08	9.08E-08	9.62E-08	9.62E-08	9.62E-08	9.62E-08	1.26E-07	1.26E-07	1.59E-07	1.59E-07
Predicted Breaking mass	15.935	15.935	15.935	15.935	27.685	27.685	27.882	27.882	36.160	36.160	43.980	43.980
Breaking Stress (Pa)	2.13E+09	2.28E+09	1.85E+09	3.62E+08	1.98E+09	2.37E+09	1.93E+09	2.63E+09	2.03E+09	2.50E+09	1.88E+09	2.19E+09
Company's value	1.72E+09	1.72E+09	1.72E+09	1.72E+09	2.82E+09	2.82E+09	2.84E+09	2.84E+09	2.82E+09	2.82E+09	2.71E+09	2.71E+09
Error in Breaking Stress	6.83E+07	9.35E+06	5.40E+06	0.00E+00	4.08E+07	9.75E+06	6.52E+07	2.55E+07	1.54E+07	2.30E+07	1.14E+08	4.05E+07

Wire Type	0.51mm (Gla)	0.51mm round	0.51mm grooved	0.54 mm (Gla)	0.54 mm round	0.6 mm (Gla)	0.6 round	0.8mm (Gla)	0.8mm round	0.85 mm (Gla)	0.85 round
Breaking Mass (kg)	35.8 38.2 34.8 36 35.2 38.5	45.8 46.25 46.1 45.2	39.7 38.5 38.9	45.8 47.4 46.5	53.1 52.1 51.3	46.4 44.9 47.3 44.4	56.2 57 54.6	94.8 93.4 94.2	113.2 107	98.2 95.2	112.4 115.2
Average breaking mass	36.42	45.84	39.03	46.57	52.17	45.75	55.93	94.13	110.10	96.70	113.80
Mass inc hook	39.22	48.64	41.83	49.37	54.97	48.55	58.73	96.93	112.90	99.50	116.60
Standard Error	0.637	0.232	0.353	0.463	0.521	0.669	0.706	0.406	3.100	1.500	1.400
Diameter (mm)	0.51	0.51	0.51	0.54	0.54	0.6	0.6	0.8	0.8	0.85	0.85
Cross section (m ²)	2.04E-07	2.04E-07	2.04E-07	2.29E-07	2.29E-07	2.83E-07	2.83E-07	5.03E-07	5.03E-07	5.67E-07	5.67E-07
Predicted Breaking mass	52.947	52.947	52.947	58.891	58.891	62.896	62.896	127.202	127.202	141.863	141.863
Breaking Stress (Pa)	1.88E+09	2.33E+09	2.01E+09	2.11E+09	2.35E+09	1.68E+09	2.04E+09	1.89E+09	2.20E+09	1.72E+09	2.01E+09
Company's value	2.54E+09	2.54E+09	2.54E+09	2.52E+09	2.52E+09	2.18E+09	2.18E+09	2.48E+09	2.48E+09	2.45E+09	2.45E+09
Error in Breaking Stress	3.06E+07	1.11E+07	1.69E+07	1.98E+07	2.23E+07	2.32E+07	2.45E+07	7.91E+06	6.04E+07	2.59E+07	2.42E+07

Appendix B: Young's Modulus Data

Vertical Measurement

Wire	Diameter (mm)	mass (kg)	length (m)	frequency (Hz)	Young's Modulus (Pa)
0.2 mm Elgiloy	0.2	2.85	6.28	2.7	1.640E+11
0.34 mm Elgiloy	0.34	6.85	6.55	3	1.756E+11
0.22 mm Malin	0.22	5.85	5.33	2.55	2.106E+11
0.30 mm Malin	0.3	7.85	5.71	2.9	2.105E+11
0.35 mm Malin	0.35	8.85	7.41	2.7	1.962E+11
0.35 California	0.35	10.35	7.56	2.553	2.093E+11
0.40 mm Malin	0.4	10.85	7.29	2.9	2.090E+11
0.42 mm Knight	0.42	10.85	7.91	2.975	2.164E+11
0.45 mm Knight	0.45	18.85	8.04	3	3.386E+11
0.51 mm Knight	0.51	17.85	7.01	2.917	2.058E+11
0.54 mm Knight	0.54	25.2	3.1	3.86	2.006E+11
0.55 mm Knight	0.55	28.6	3.47	3.443	1.955E+11
0.6 mm Knight	0.6	32.2	2.78	3.6	1.620E+11
0.8 mm Knight	0.8	28.4	7.78	3.425	2.036E+11
0.85mm Knight	0.85	32.5	8.05	3.2	1.864E+11

Rotational Measurement

Wire	r of wire (m)	Moment of Inertia	length (m)	frequency	Young's modulus	% diff
0.2 mm Elgiloy	0.0001	1.33E-04	0.135	0.120	1.69E+11	3.13
0.34 mm Elgiloy	0.00017	1.33E-04	0.125	0.391	1.98E+11	12.58
0.22 mm Malin	0.00011	1.33E-04	0.25	0.126	2.33E+11	10.66
0.30 mm Malin	0.00015	1.33E-04	0.156	0.275	2.02E+11	4.15
0.35 mm Malin	0.000175	1.33E-04	0.203	0.313	1.82E+11	7.02
0.35 California	0.000175	1.33E-04	0.2	0.313	1.80E+11	14.13
0.40 mm Malin	0.0002	1.33E-04	0.182	0.434	1.85E+11	11.60
0.42 mm Knight	0.00021	1.33E-04	0.18	0.499	1.99E+11	8.17
0.45 mm Knight	0.000225	1.33E-04	0.162	0.799	3.48E+11	2.88
0.51 mm Knight	0.000255	1.33E-04	0.146	0.769	1.76E+11	14.32
0.54 mm Knight	0.00027	1.33E-04	0.153	0.894	1.99E+11	1.06
0.55 mm Knight	0.000275	1.33E-04	0.167	0.865	1.89E+11	3.47
0.6 mm Knight	0.0003	1.33E-04	0.141	1.064	1.70E+11	4.94
0.8 mm Knight	0.0004	1.33E-04	0.182	1.786	1.96E+11	3.91
0.85mm Knight	0.000425	1.33E-04	0.167	1.852	1.51E+11	18.73

Appendix C: Upper-Mass Bending Model Results

MIT PROTOTYPE QUAD

DEFLECTION CALCULATOR for MASSES LOADED WITH BLADES

AUTHOR: - Dan Mason, masond2@rpi.edu

SURF Student, Caltech 2003 with Calum Torrie

VERSION: - 1.1

DATE: - 15th April 2003

SUMMARY: **The following is a draft version of a deflection calculator that allows the deflection of a bar, the main section of an upper mass, wrt to a blade .The report on this and other related topics can be found at the link below**

KEY: - SHEET 1: DEFLECTION CALCULATOR

SHEET 2: NOTES on INPUTS

LINK: [SURF FINAL REPORT, 16th April 2003](#)

Moment of Inertia Calculator	
Mass of Upper mass	0.4
Mass of Blade	0.1
height of clamps	0.022
d1 upper mass to cm	0.0044
d2 blade to cm	0.0176
MOI, blade and mass	3.640E-08
MOI, mass only	5.120E-09

Deflection Calculator

Inputs		mm	m
a	depth of clamps	30	0.03
b	width of upper mass	120	0.12
l	1/2 length of upper mass	250	0.25
h	thickness of upper mass	8	0.008
c	length of blade	450	0.45
	width of blade	25	0.025
	thickness of blade	2.3	0.0023
d	mass overhang	N/R	0
m	mass applied		37.5 kg

Calculations

w	Force Applied	367.875
R	Reaction Force (Down Push)	-10668.38
F	Reaction (Push Up)	10300.5
I	Moment of Inertia	5.12E-09
E	Modulus of Elasticity	6.89E+10 aluminum

Models

Force Model

Deflection Down -107.339 mm

Deflection Up 114.220 mm

Overall deflection (Eq. 1) 6.8815 mm

Force/Moment Model

Force -5.431 mm

Moment 14.665 mm

Overall Deflection (Eq. 2) 9.233 mm

Average: 8.05742 mm

SECOND-GENERATION PROTOTYPE QUAD LIGHTEST CONFIGURATION, ALUMINUM

DEFLECTION CALCULATOR for MASSES LOADED WITH BLADES

AUTHOR: - Dan Mason, masond2@rpi.edu

SURF Student, Caltech 2003 with Calum Torrie

VERSION: - **1.1**

DATE: - 15th April 2003

SUMMARY: **The following is a draft version of a deflection calculator that allows the deflection of a bar, the main section of an upper mass, wrt to a blade .The report on this and other related topics can be found at the link below**

KEY: - SHEET 1: DEFLECTION CALCULATOR

SHEET 2: NOTES on INPUTS

LINK: [SURF FINAL REPORT, 16th April 2003](#)

Deflection Calculator			
Inputs		mm	m
a	depth of clamps	30	0.03
b	width of upper mass	120	0.12
l	1/2 length of upper mass	250	0.25
h	thickness of upper mass	18	0.018
c	length of blade	450	0.45
	width of blade	25	0.025
	thickness of blade	2.3	0.0023
d	mass overhang	N/R	0
m	mass applied		53 kg

Calculations

w	Force Applied	519.93
R	Reaction Force (Down Push)	-15077.97
F	Reaction (Push Up)	14558.04
I	Moment of Inertia	5.83E-08
E	Modulus of Elasticity	6.89E+10 aluminum

Moment of Inertia Calculator

Mass of Upper mass	0.4
Mass of Blade	0.1
height of clamps	0.022
d1 upper mass to cm	0.0044
d2 blade to cm	0.0176
MOI, blade and mass	5.963E-08
MOI, mass only	5.832E-08

Models

Force Model

Deflection Down -13.318 mm

Deflection Up 14.172 mm

Overall deflection (Eq. 1) 0.8538 mm

Force/Moment Model

Force -0.674 mm

Moment 1.820 mm

Overall Deflection (Eq. 2) 1.146 mm

Average: 0.99975 mm

SECOND-GENERATION PROTOTYPE QUAD HEAVIEST CONFIGURATION, ALUMINUM

DEFLECTION CALCULATOR for MASSES LOADED WITH BLADES

AUTHOR: - Dan Mason, masond2@rpi.edu

SURF Student, Caltech 2003 with Calum Torrie

VERSION: - **1.1**

DATE: - 15th April 2003

SUMMARY: **The following is a draft version of a deflection calculator that allows the deflection of a bar, the main section of an upper mass, wrt to a blade .The report on this and other related topics can be found at the link below**

KEY: - SHEET 1: DEFLECTION CALCULATOR

SHEET 2: NOTES on INPUTS

LINK: [SURF FINAL REPORT, 16th April 2003](#)

Deflection Calculator			
Inputs		mm	m
a	depth of clamps	30	0.03
b	width of upper mass	120	0.12
l	1/2 length of upper mass	250	0.25
h	thickness of upper mass	21	0.021
c	length of blade	450	0.45
	width of blade	25	0.025
	thickness of blade	2.3	0.0023
d	mass overhang	N/R	0
m	mass applied		76 kg

Calculations

w	Force Applied	745.56
R	Reaction Force (Down Push)	-21621.24
F	Reaction (Push Up)	20875.68
I	Moment of Inertia	9.26E-08
E	Modulus of Elasticity	6.89E+10 aluminum

Moment of Inertia Calculator	
Mass of Upper mass	0.4
Mass of Blade	0.1
height of clamps	0.022
d1 upper mass to cm	0.0044
d2 blade to cm	0.0176
MOI, blade and mass	6.660E-08
MOI, mass only	9.261E-08

Models

Force Model

Deflection Down -12.027 mm

Deflection Up 12.798 mm

Overall deflection (Eq. 1) 0.7710 mm

Force/Moment Model

Force -0.609 mm

Moment 1.643 mm

Overall Deflection (Eq. 2) 1.035 mm

Average: 0.90280 mm

SECOND-GENERATION PROTOTYPE QUAD LIGHTEST CONFIGURATION, STAINLESS STEEL

DEFLECTION CALCULATOR for MASSES LOADED WITH BLADES

AUTHOR: - Dan Mason, masond2@rpi.edu

SURF Student, Caltech 2003 with Calum Torrie

VERSION: - **1.1**

DATE: - 15th April 2003

SUMMARY: **The following is a draft version of a deflection calculator that allows the deflection of a bar, the main section of an upper mass, wrt to a blade .The report on this and other related topics can be found at the link below**

KEY: - SHEET 1: DEFLECTION CALCULATOR

SHEET 2: NOTES on INPUTS

LINK: [SURF FINAL REPORT, 16th April 2003](#)

Deflection Calculator			
Inputs		mm	m
a	depth of clamps	30	0.03
b	width of upper mass	120	0.12
l	1/2 length of upper mass	250	0.25
h	thickness of upper mass	13	0.013
c	length of blade	450	0.45
	width of blade	25	0.025
	thickness of blade	2.3	0.0023
d	mass overhang	N/R	0
m	mass applied		53 kg

Calculations

w	Force Applied	519.93	
R	Reaction Force (Down Push)	-15077.97	
F	Reaction (Push Up)	14558.04	
I	Moment of Inertia	2.20E-08	
E	Modulus of Elasticity	1.93E+11	stainless steel

Moment of Inertia Calculator

Mass of Upper mass	0.4
Mass of Blade	0.1
height of clamps	0.022
d1 upper mass to cm	0.0044
d2 blade to cm	0.0176
MOI, blade and mass	4.801E-08
MOI, mass only	2.197E-08

Models

Force Model

Deflection Down -12.621 mm

Deflection Up 13.430 mm

Overall deflection (Eq. 1) 0.8092 mm

Force/Moment Model

Force -0.639 mm

Moment 1.724 mm

Overall Deflection (Eq. 2) 1.086 mm

Average: 0.94742 mm

SECOND-GENERATION PROTOTYPE QUAD HEAVIEST CONFIGURATION, STAINLESS STEEL

DEFLECTION CALCULATOR for MASSES LOADED WITH BLADES

AUTHOR: - Dan Mason, masond2@rpi.edu

SURF Student, Caltech 2003 with Calum Torrie

VERSION: - **1.1**

DATE: - 15th April 2003

SUMMARY: **The following is a draft version of a deflection calculator that allows the deflection of a bar, the main section of an upper mass, wrt to a blade .The report on this and other related topics can be found at the link below**

KEY: - SHEET 1: DEFLECTION CALCULATOR

SHEET 2: NOTES on INPUTS

LINK: [SURF FINAL REPORT, 16th April 2003](#)

Deflection Calculator			
Inputs		mm	m
a	depth of clamps	30	0.03
b	width of upper mass	120	0.12
l	1/2 length of upper mass	250	0.25
h	thickness of upper mass	15	0.015
c	length of blade	450	0.45
	width of blade	25	0.025
	thickness of blade	2.3	0.0023
d	mass overhang	N/R	0
m	mass applied		76 kg

Calculations

w	Force Applied	745.56	
R	Reaction Force (Down Push)	-21621.24	
F	Reaction (Push Up)	20875.68	
I	Moment of Inertia	3.38E-08	
E	Modulus of Elasticity	1.93E+11	stainless steel

Moment of Inertia Calculator

Mass of Upper mass	0.4
Mass of Blade	0.1
height of clamps	0.022
d1 upper mass to cm	0.0044
d2 blade to cm	0.0176
MOI, blade and mass	5.266E-08
MOI, mass only	3.375E-08

Models

Force Model

Deflection Down -11.781 mm

Deflection Up 12.537 mm

Overall deflection (Eq. 1) 0.7553 mm

Force/Moment Model

Force -0.596 mm

Moment 1.610 mm

Overall Deflection (Eq. 2) 1.013 mm

Average: 0.88438 mm

Appendix D: Cold-Welding Data

4-40 Bolts

Stainless Plates

		Description	5 in lb	8 in lb	12 in lb	16 in lb	20 in lb	
Stainless Steel	UNC-2B	Row 1	sst/sst unc-2b	broken	-	-	-	-
		Row 2	sst/sst unc-2b	1	4	-	-	-
		Row 3	sst/sst unc-2b	1	4	-	-	-
		Row 4	sst/sst unc-2b	1	4	-	-	-
		Row 5	sst/sst unc-2b	1	4	-	-	-
		Row 6	sst/sst unc-2b	1	4	-	-	-
	UNC-1B	Row 1	sst/sst unc-1b	1	1	2	1	2
		Row 2	sst/sst unc-1b	1	1	3	4	-
		Row 3	sst/sst unc-1b	1	1	1	1	2
		Row 4	sst/sst unc-1b	1	1	1	1	broken
		Row 5	sst/sst unc-1b	1	4	-	-	-
		Row 6	sst/sst unc-1b	1	1	4	-	-
	OVERSIZE	Row 1	sst/sst oversize	1	1	1	1	2
		Row 2	sst/sst oversize	1	1	2	2	2
		Row 3	sst/sst oversize	1	1	4	-	-
		Row 4	sst/sst oversize	1	1	1	1	1
		Row 5	sst/sst oversize	-	-	-	-	-
		Row 6	sst/sst oversize	1	1	1	1	1

		Description	5 in lb	8 in lb	12 in lb	16 in lb	20 in lb	
Silver Plated	UNC-2B	Row 1	ag/sst unc-2b	2	3	3	3	breaks at 20
		Row 2	ag/sst unc-2b	2	3	3	3	breaks at 17
		Row 3	ag/sst unc-2b	3	3	3	3	breaks at 17
		Row 4	ag/sst unc-2b	1	2	2	3	breaks at 19
		Row 5	ag/sst unc-2b	2	2	3	3	breaks at 20
		Row 6	ag/sst unc-2b	3	3	3	3	breaks at 19
	UNC-1B	Row 1	ag/sst unc-1b	1	1	1	1	break 19-20
		Row 2	ag/sst unc-1b	1	1	1	1	"
		Row 3	ag/sst unc-1b	1	1	1	1	"
		Row 4	ag/sst unc-1b	2	2	2	2	"
		Row 5	ag/sst unc-1b	1	1	1	1	"
		Row 6	ag/sst unc-1b	1	1	1	1	"
	OVERSIZE	Row 1	ag/sst oversize	1	1	1	1	break 18-20
		Row 2	ag/sst oversize	1	1	1	1	"
		Row 3	ag/sst oversize	1	1	1	1	"
		Row 4	ag/sst oversize	1	1	1	1	"
		Row 5	ag/sst oversize	1	1	1	1	"
		Row 6	ag/sst oversize	1	1	1	1	"

4-40 Bolts

Aluminum Plates

		Description	5 in lb	8 in lb	12 in lb	16 in lb	20 in lb	
Stainless Steel	UNC-2B	Row 1	sst/al unc-2b	1	1	1	1	1
		Row 2	sst/al unc-2b	1	1	1	1	1
		Row 3	sst/al unc-2b	1	1	2	2	2
		Row 4	sst/al unc-2b	1	2	2	2	2
		Row 5	sst/al unc-2b	1	2	2	2	2
		Row 6	sst/al unc-2b	1	1	2	2	2
	UNC-1B	Row 1	sst/al unc-1b	1	1	1	1	1
		Row 2	sst/al unc-1b	1	1	1	1	1
		Row 3	sst/al unc-1b	1	1	1	1	1
		Row 4	sst/al unc-1b	1	1	1	1	1
		Row 5	sst/al unc-1b	1	1	1	1	1
		Row 6	sst/al unc-1b	1	1	1	1	1
	OVERSIZE	Row 1	sst/al oversize	1	1	1	1	1
		Row 2	sst/al oversize	1	1	1	1	1
		Row 3	sst/al oversize	1	1	1	1	1
		Row 4	sst/al oversize	1	1	1	1	1
		Row 5	sst/al oversize	1	1	1	1	1
		Row 6	sst/al oversize	1	1	1	1	1

		Description	5 in lb	8 in lb	12 in lb	16 in lb	20 in lb	
Silver Plated	UNC-2B	Row 1	ag/al unc-2b	2	4	-	-	-
		Row 2	ag/al unc-2b	3	4	-	-	-
		Row 3	ag/al unc-2b	2	4	-	-	-
		Row 4	ag/al unc-2b	2	4	-	-	-
		Row 5	ag/al unc-2b	3	4	-	-	-
		Row 6	ag/al unc-2b	3	4	-	-	-
	UNC-1B	Row 1	ag/al unc-1b	1	1	stripped	-	-
		Row 2	ag/al unc-1b	1	1	stripped	-	-
		Row 3	ag/al unc-1b	1	1	1	1	1
		Row 4	ag/al unc-1b	1	1	1	1	1
		Row 5	ag/al unc-1b	1	1	2	stripped	-
		Row 6	ag/al unc-1b	3	4	-	-	-
	OVERSIZE	Row 1	ag/al oversize	1	1	1	1	1
		Row 2	ag/al oversize	1	1	1	1	1
		Row 3	ag/al oversize	1	1	1	1	1
		Row 4	ag/al oversize	1	1	1	1	1
		Row 5	ag/al oversize	1	1	1	1	1
		Row 6	ag/al oversize	1	1	1	1	1

1/4 - 20 Bolts

Stainless Plates

		Description	12 in lb	20 in lb	40 in lb	60 in lb	80 in lb
Stainless Steel	UNC-2B	Row 1 sst/sst unc-2b	1	4	-	-	-
		Row 2 sst/sst unc-2b	1	4	-	-	-
		Row 3 sst/sst unc-2b	1	4	-	-	-
		Row 4 sst/sst unc-2b	1	3	4	-	-
		Row 5 sst/sst unc-2b	2	4	-	-	-
		Row 6 sst/sst unc-2b	2	4	-	-	-
	UNC-1B	Row 1 sst/sst unc-1b	1	2	4	-	-
		Row 2 sst/sst unc-1b	1	4	-	-	-
		Row 3 sst/sst unc-1b	1	4	-	-	-
		Row 4 sst/sst unc-1b	1	4	-	-	-
		Row 5 sst/sst unc-1b	2	4	-	-	-
		Row 6 sst/sst unc-1b	4	-	-	-	-
	OVERSIZE	Row 1 sst/sst oversize	1	1	1	1	1
		Row 2 sst/sst oversize	1	1	1	1	1
		Row 3 sst/sst oversize	1	1	1	1	1
		Row 4 sst/sst oversize	1	1	1	1	1
		Row 5 sst/sst oversize	1	1	1	1	1
		Row 6 sst/sst oversize	1	1	1	1	1

		Description	12 in lb	20 in lb	40 in lb	60 in lb	80 in lb
Silver Plated	UNC-2B	Row 1 ag/sst unc-2b	1	1	2	3	3
		Row 2 ag/sst unc-2b	1	2	2	3	3
		Row 3 ag/sst unc-2b	1	2	2	3	3
		Row 4 ag/sst unc-2b	1	2	2	3	3
		Row 5 ag/sst unc-2b	1	1	2	3	3
		Row 6 ag/sst unc-2b	1	1	2	3	3
	UNC-1B	Row 1 ag/sst unc-1b	2	2	2	3	3
		Row 2 ag/sst unc-1b	1	2	2	2	2
		Row 3 ag/sst unc-1b	1	2	3	3	3
		Row 4 ag/sst unc-1b	2	2	2	2	2
		Row 5 ag/sst unc-1b	1	2	3	3	3
		Row 6 ag/sst unc-1b	1	1	2	3	3
	OVERSIZE	Row 1 ag/sst oversize	1	1	1	1	1
		Row 2 ag/sst oversize	1	1	1	1	1
		Row 3 ag/sst oversize	1	1	1	1	1
		Row 4 ag/sst oversize	1	1	1	1	1
		Row 5 ag/sst oversize	1	1	1	1	1
		Row 6 ag/sst oversize	1	1	1	1	1

1/4 - 20 Bolts

Aluminum plates

		Description	12 in lb	20 in lb	40 in lb	60 in lb	80 in lb
Stainless Steel	UNC-2B	Row 1 sst/al unc-2b	2	2	2	2	2
		Row 2 sst/al unc-2b	2	2	2	2	3
		Row 3 sst/al unc-2b	1	2	2	2	2
		Row 4 sst/al unc-2b	1	1	2	2	2
		Row 5 sst/al unc-2b	1	2	2	2	2
		Row 6 sst/al unc-2b	1	2	2	2	2
	UNC-1B	Row 1 sst/al unc-1b	1	1	1	1	2
		Row 2 sst/al unc-1b	1	2	2	2	2
		Row 3 sst/al unc-1b	1	1	1	2	2
		Row 4 sst/al unc-1b	1	1	1	1	1
		Row 5 sst/al unc-1b	1	1	1	1	1
		Row 6 sst/al unc-1b	1	1	1	1	1
	OVERSIZE	Row 1 sst/al oversize	1	1	1	1	1
		Row 2 sst/al oversize	1	1	1	1	1
		Row 3 sst/al oversize	1	1	1	1	1
		Row 4 sst/al oversize	1	1	1	1	1
		Row 5 sst/al oversize	1	1	1	1	1
		Row 6 sst/al oversize	1	1	1	1	1

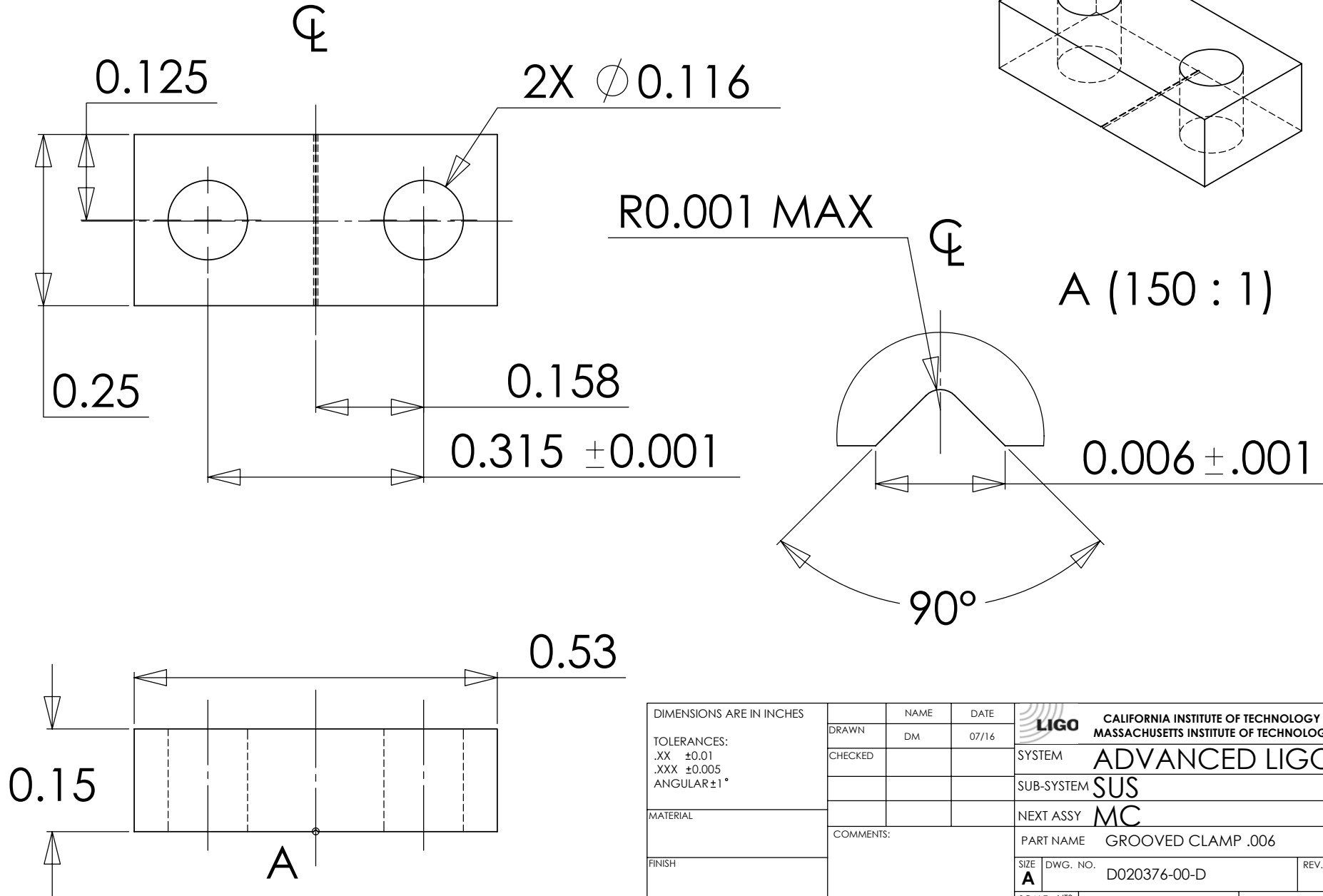
		Description	12 in lb	20 in lb	40 in lb	60 in lb	80 in lb
Silver Plated	UNC-2B	Row 1 ag/al unc-2b	3	3	3	4	-
		Row 2 ag/al unc-2b	3	3	4	-	-
		Row 3 ag/al unc-2b	3	3	3	4	-
		Row 4 ag/al unc-2b	2	2	2	3	4
		Row 5 ag/al unc-2b	2	3	3	4	-
		Row 6 ag/al unc-2b	2	2	3	4	-
	UNC-1B	Row 1 ag/al unc-1b	2	3	4	-	-
		Row 2 ag/al unc-1b	2	3	3	3	3
		Row 3 ag/al unc-1b	1	2	2	2	3
		Row 4 ag/al unc-1b	2	2	2	4	-
		Row 5 ag/al unc-1b	2	3	3	3	3
		Row 6 ag/al unc-1b	1	2	3	3	3
	OVERSIZE	Row 1 ag/al oversize	1	1	1	1	1
		Row 2 ag/al oversize	1	1	1	1	1
		Row 3 ag/al oversize	1	1	1	1	1
		Row 4 ag/al oversize	1	1	2	3	3
		Row 5 ag/al oversize	1	1	1	1	1
		Row 6 ag/al oversize	1	1	1	1	1

NOTES: (UNLESS OTHERWISE SPECIFIED)

1. DIMENSIONS IN INCHES

2. ALL MACHINING FLUIDS SHALL BE WATER SOLUBLE AND FREE OF SULFUR, CHLORINE AND SILICONE, SUCH AS CINCINNATI MILACRON'S CIMTECH 410 (STAINLESS STEEL)

REV.	DATE	DCN #	DRAWING TREE #



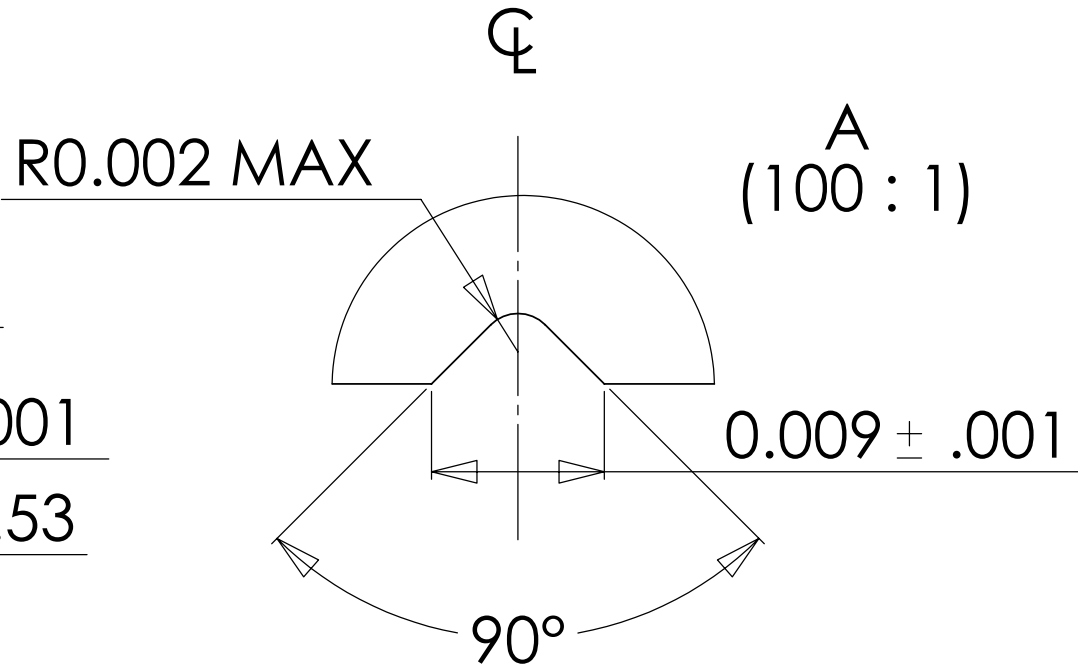
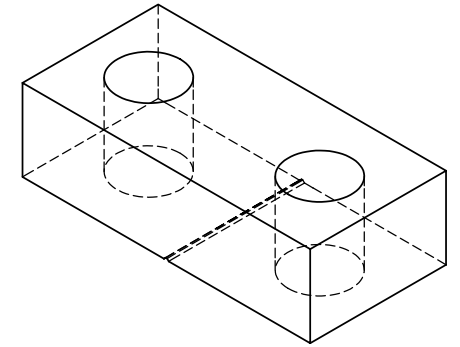
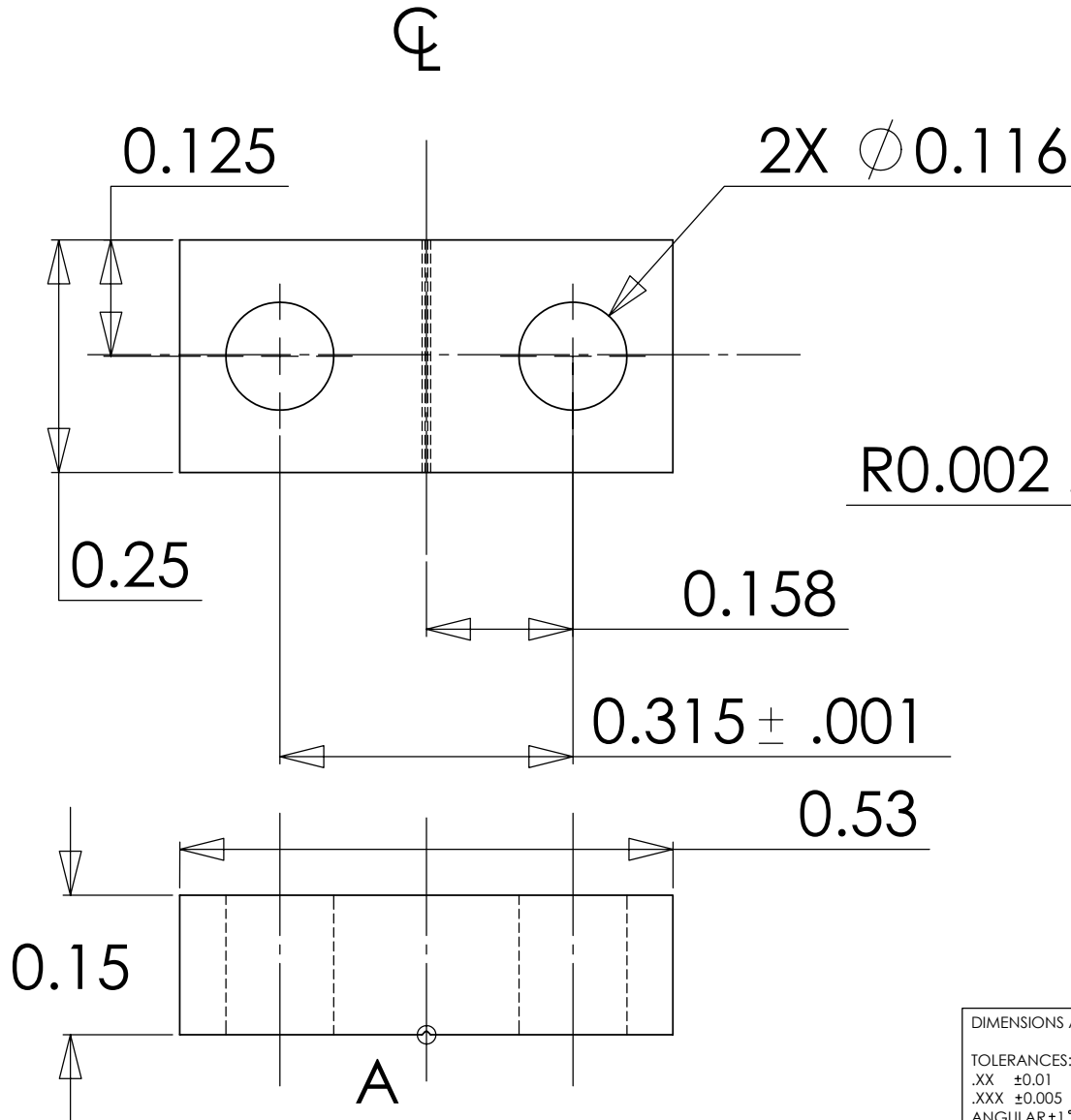
DIMENSIONS ARE IN INCHES		NAME	DATE	CALIFORNIA INSTITUTE OF TECHNOLOGY MASSACHUSETTS INSTITUTE OF TECHNOLOGY
TOLERANCES: .XX ±0.01 .XXX ±0.005 ANGULAR±1°		DM	07/16	
DRAWN				SYSTEM ADVANCED LIGO
CHECKED				SUB-SYSTEM SUS
MATERIAL				NEXT ASSY MC
FINISH		COMMENTS:		PART NAME GROOVED CLAMP .006
		SCALE: NTS		SIZE A DWG. NO. D020376-00-D REV.
				SHEET 1 OF 1


NOTES: (UNLESS OTHERWISE SPECIFIED)

1. DIMENSIONS IN INCHES

2. ALL MACHINING FLUIDS SHALL BE WATER SOLUBLE AND FREE OF SULFUR, CHLORINE AND SILICONE, SUCH AS CINCINNATI MILACRON'S CIMTECH 410 (STAINLESS STEEL)

REV.	DATE	DCN #	DRAWING TREE #



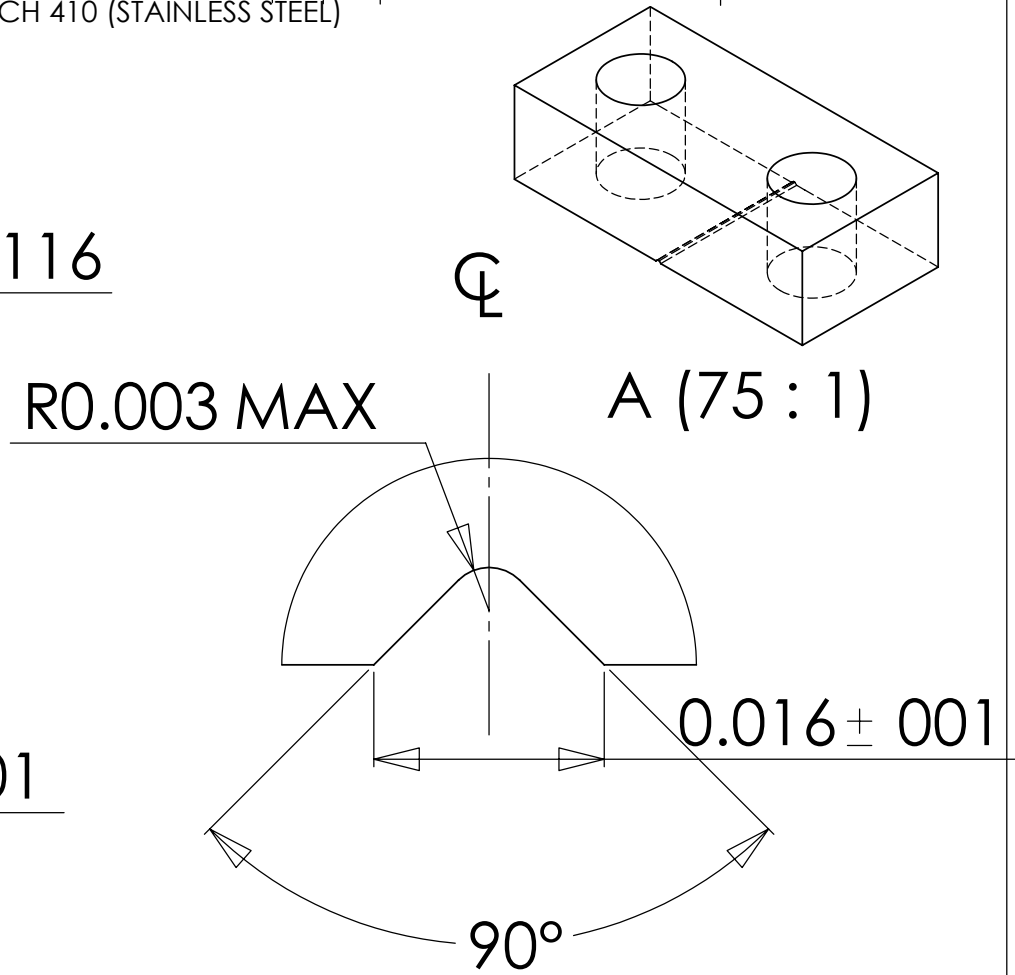
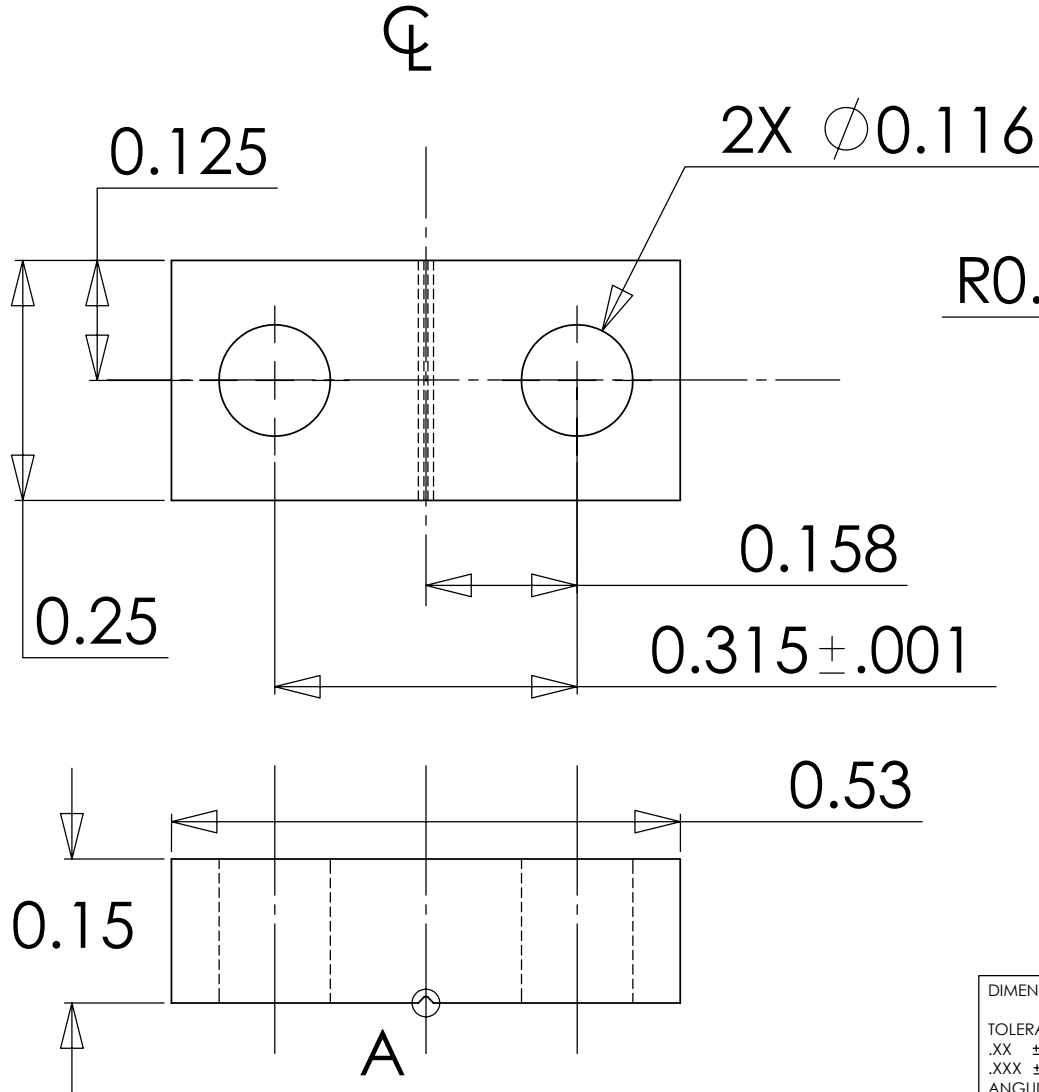
DIMENSIONS ARE IN INCHES		NAME	DATE	 CALIFORNIA INSTITUTE OF TECHNOLOGY MASSACHUSETTS INSTITUTE OF TECHNOLOGY
TOLERANCES: .XX ±0.01 .XXX ±0.005 ANGULAR ±1°		DM	07/16	
DRAWN				SYSTEM ADVANCED LIGO
CHECKED				SUB-SYSTEM SUS
MATERIAL				NEXT ASSY MC
FINISH				PART NAME GROOVED CLAMP .009
COMMENTS:				SIZE A DWG. NO. D020377-00-D REV.
				SCALE: NTS SHEET 1 OF 1


NOTES: (UNLESS OTHERWISE SPECIFIED)

1. DIMENSIONS IN INCHES

2. ALL MACHINING FLUIDS SHALL BE WATER SOLUBLE AND FREE OF SULFUR, CHLORINE AND SILICONE, SUCH AS CINCINNATI MILACRON'S CIMTECH 410 (STAINLESS STEEL)

REV.	DATE	DCN #	DRAWING TREE #



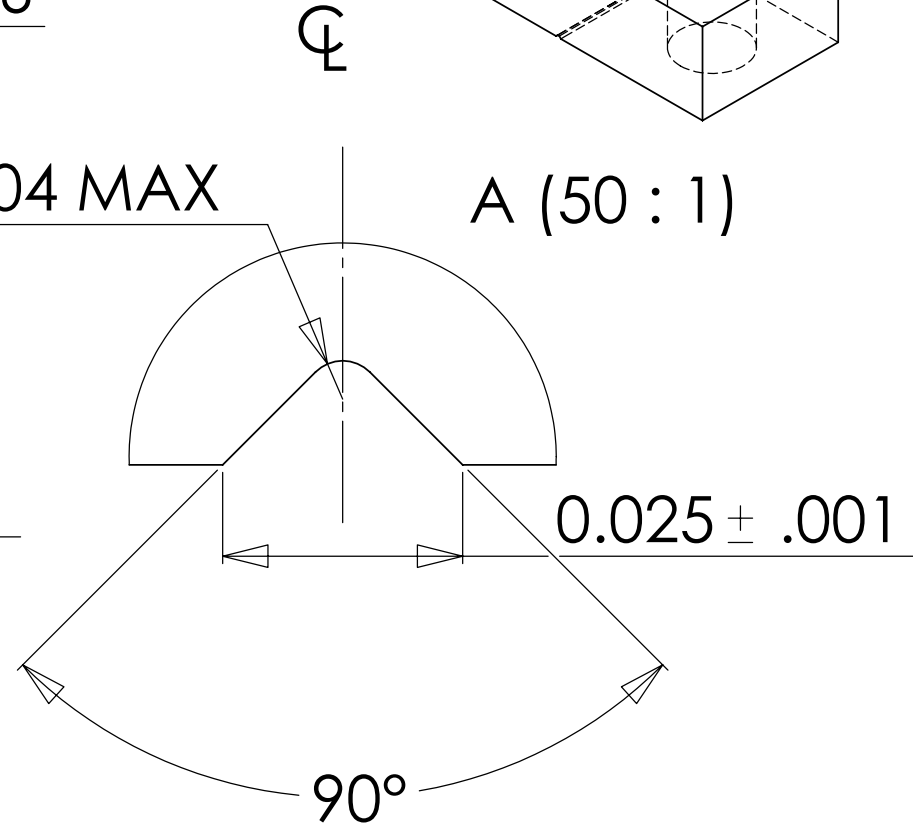
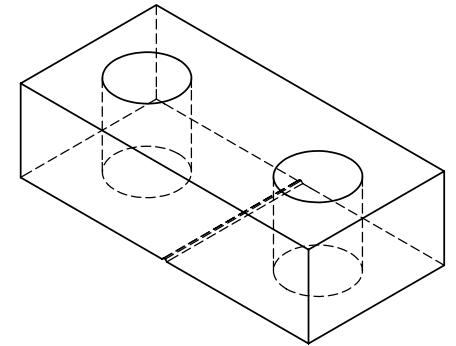
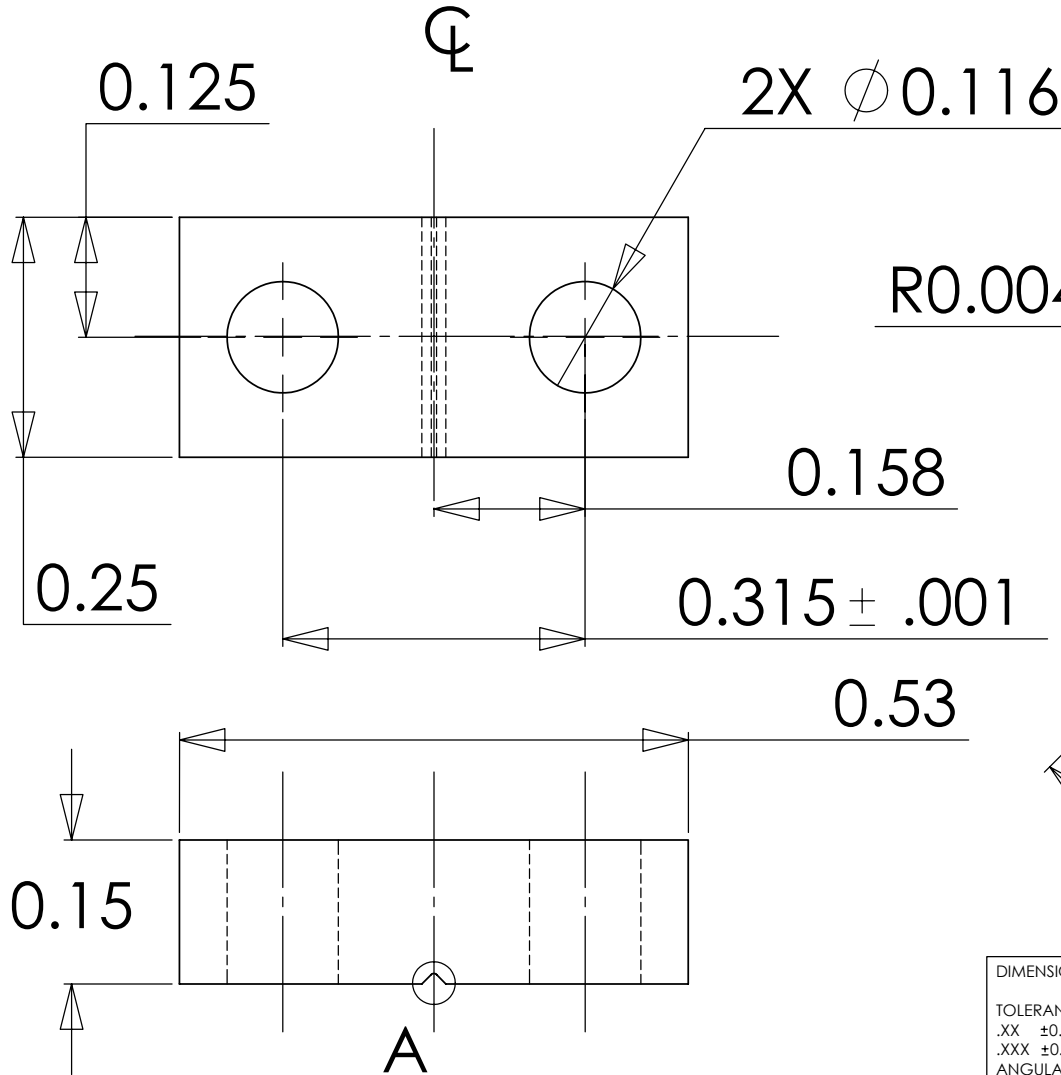
DIMENSIONS ARE IN INCHES		NAME	DATE	 CALIFORNIA INSTITUTE OF TECHNOLOGY MASSACHUSETTS INSTITUTE OF TECHNOLOGY
TOLERANCES: .XX ±0.01 .XXX ±0.005 ANGULAR ±1°		DM	07/16	
DRAWN				SYSTEM ADVANCED LIGO
CHECKED				SUB-SYSTEM SUS
MATERIAL				NEXT ASSY MC
FINISH		COMMENTS:		PART NAME GROOVED CLAMP .016
		SIZE A	DWG. NO. D020378-00-D	REV.
		SCALE: NTS		SHEET 1 OF 1


NOTES: (UNLESS OTHERWISE SPECIFIED)

1. DIMENSIONS IN INCHES

2. ALL MACHINING FLUIDS SHALL BE WATER SOLUBLE AND FREE OF SULFUR, CHLORINE AND SILICONE, SUCH AS CINCINNATI MILACRON'S CIMTECH 410 (STAINLESS STEEL)

REV.	DATE	DCN #	DRAWING TREE #



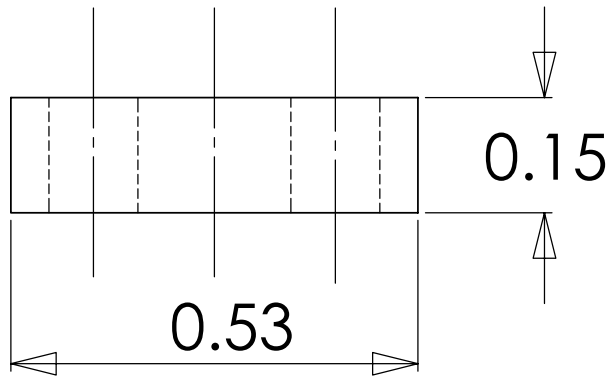
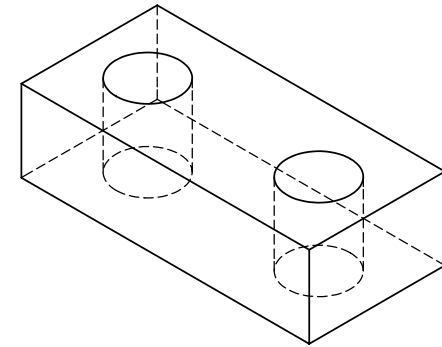
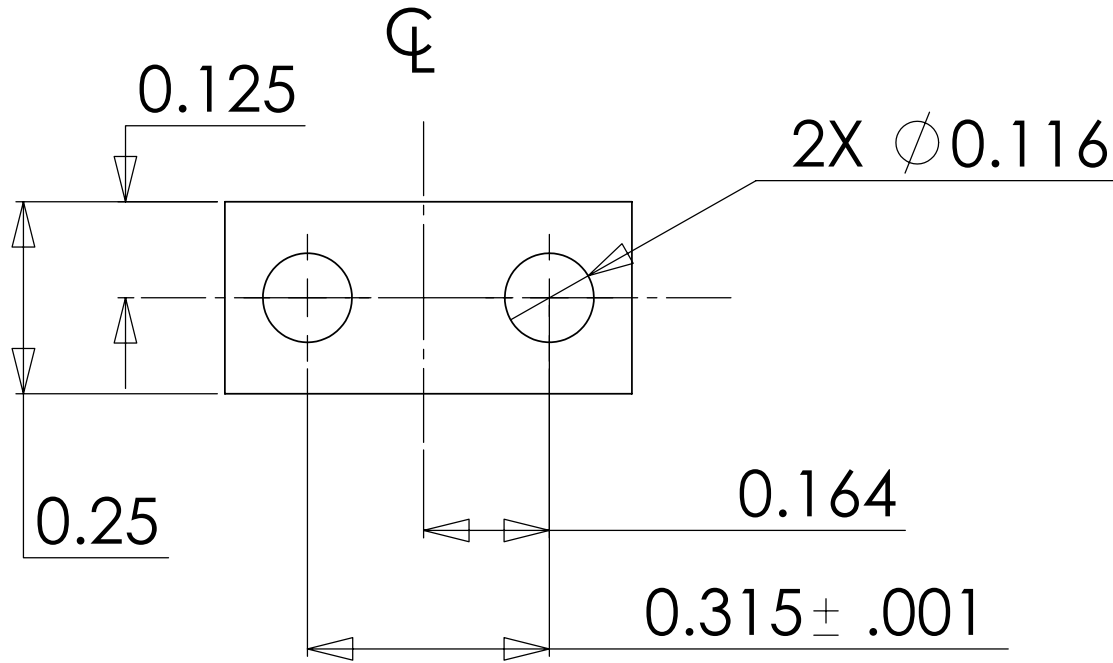
DIMENSIONS ARE IN INCHES		NAME	DATE	 CALIFORNIA INSTITUTE OF TECHNOLOGY MASSACHUSETTS INSTITUTE OF TECHNOLOGY
TOLERANCES: .XX ±0.01 .XXX ±0.005 ANGULAR ±1°		DM	07/16	
DRAWN				SYSTEM ADVANCED LIGO
CHECKED				SUB-SYSTEM SUS
MATERIAL				NEXT ASSY MC
FINISH				PART NAME GROOVED CLAMP .025
COMMENTS:				SIZE A DWG. NO. D020379-00-D REV.
				SCALE: NTS SHEET 1 OF 1


NOTES: (UNLESS OTHERWISE SPECIFIED)

1. DIMENSIONS IN INCHES

2. ALL MACHINING FLUIDS SHALL BE WATER SOLUBLE AND FREE OF SULFUR, CHLORINE AND SILICONE, SUCH AS CINCINNATI MILACRON'S CIMTECH 410 (STAINLESS STEEL)

REV.	DATE	DCN #	DRAWING TREE #



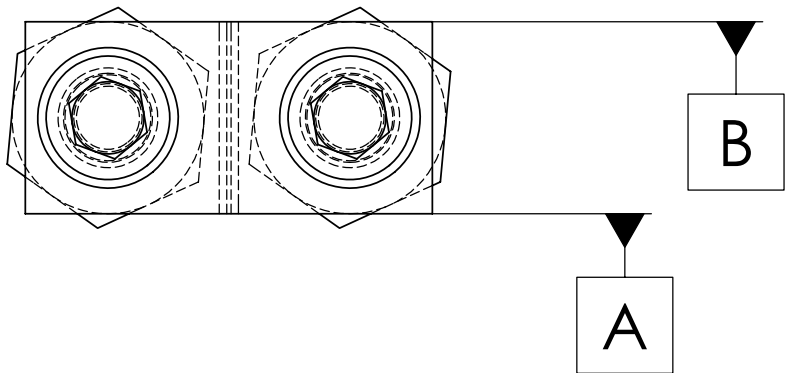
DIMENSIONS ARE IN INCHES		NAME	DATE	 CALIFORNIA INSTITUTE OF TECHNOLOGY MASSACHUSETTS INSTITUTE OF TECHNOLOGY
TOLERANCES: .XX ±0.01 .XXX ±0.005 ANGULAR ±1°		DM	07/16	
DRAWN				SYSTEM ADVANCED LIGO
CHECKED				SUB-SYSTEM SUS
MATERIAL				NEXT ASSY MC
FINISH		COMMENTS:		PART NAME MACHINED CLAMP BASE
				SIZE A DWG. NO. D020380-00-D REV.
				SCALE: 4:1 SHEET 1 OF 1

NOTES: (UNLESS OTHERWISE SPECIFIED)

1. FLY CUT DATUM -A- AND -B- SURFACE TO ACHIEVE FLATNESS OF .001

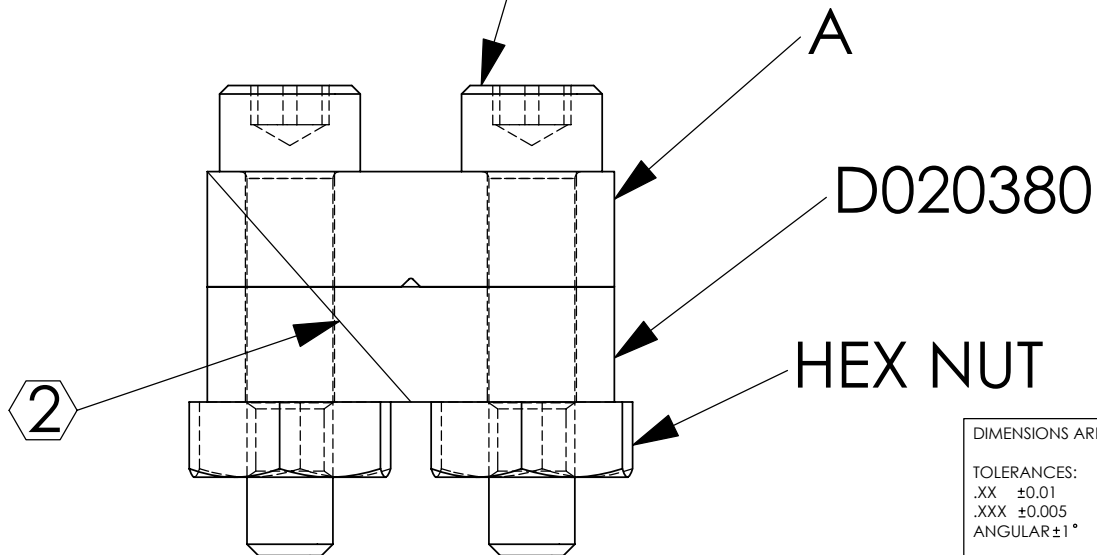
② SCRIBE OR ETCH LINE APPROX AS SHOWN .02 DEEP .02 WIDE AFTER FLYCUTTING AND PRIOR TO ASSEMBLY


REV.	DATE	DCN #	DRAWING TREE #



DASH NO.	A
-1	D020376
-2	D020377
-3	D020378
-4	D020379

4-40 SCREW

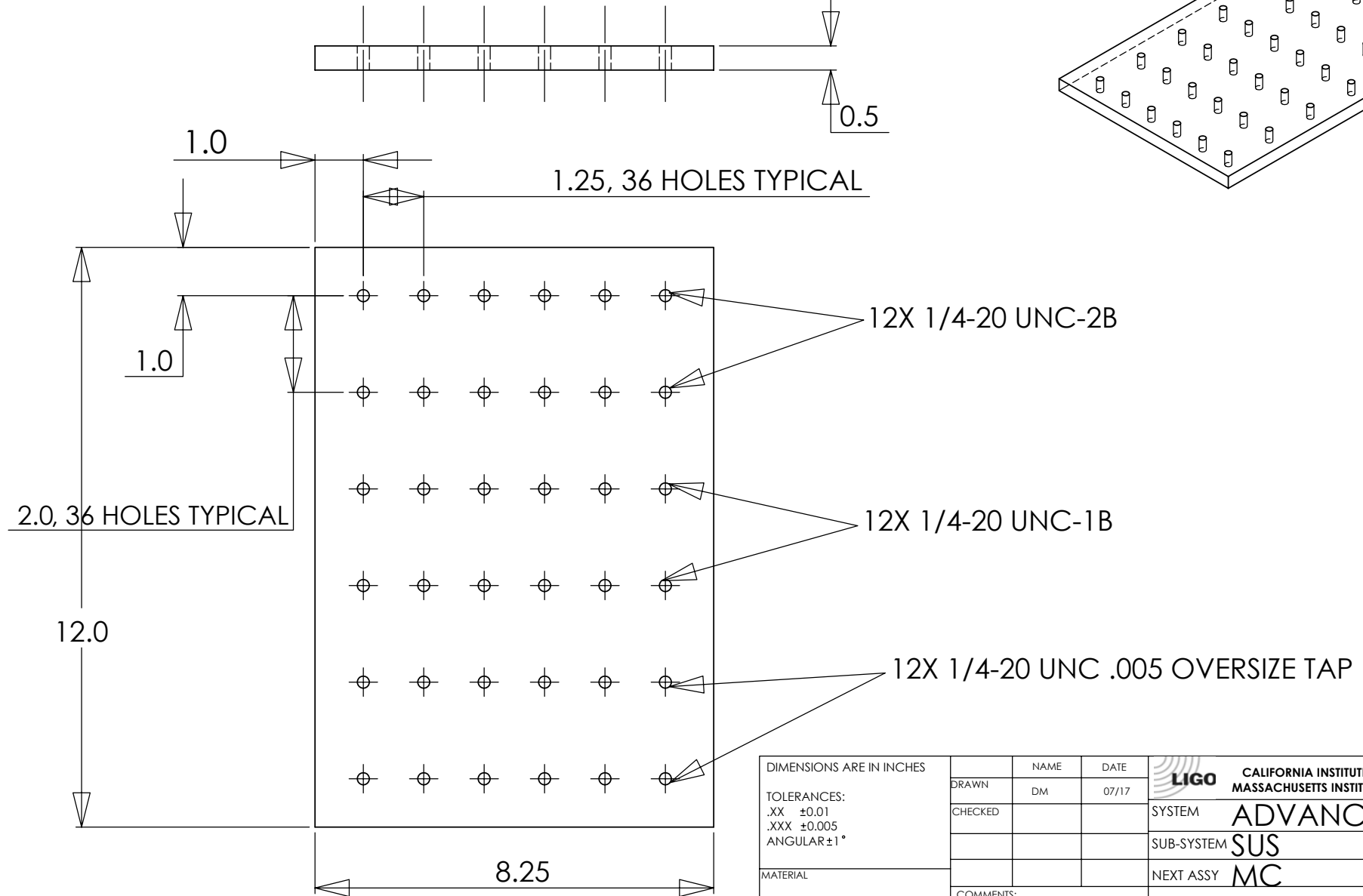
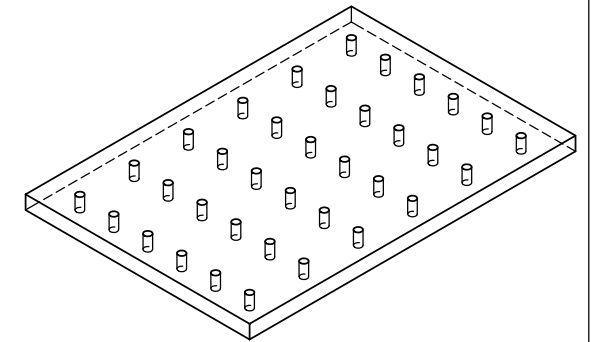


DIMENSIONS ARE IN INCHES		NAME	DATE	 CALIFORNIA INSTITUTE OF TECHNOLOGY MASSACHUSETTS INSTITUTE OF TECHNOLOGY
TOLERANCES: .XX ±0.01 .XXX ±0.005 ANGULAR±1°		DM	07/16	
MATERIAL		CHECKED		SYSTEM ADVANCED LIGO
FINISH		COMMENTS:		SUB-SYSTEM SUS
				NEXT ASSY MC
				PART NAME MACHINED CLAMP ASSEMBLY
		SIZE A	DWG. NO. D020381-00-D	REV.
		SCALE: NTS	SHEET 1 OF 1	

NOTES: (UNLESS OTHERWISE SPECIFIED)

1. DIMENSIONS IN INCHES
2. REMOVE ALL SHARP EDGES, R.02 MIN
3. ALL MACHINING FLUIDS SHALL BE WATER SOLUBLE AND FREE OF SULFUR, CHLORINE AND SILICONE, SUCH AS CINCINNATI MILACRON'S CIMTECH 410 (STAINLESS STEEL)
4. QUANTITY 2: ONE EACH OF MATERIALS 6061-T6-AL AND STAINLESS STEEL 300

REV.	DATE	DCN #	DRAWING TREE #

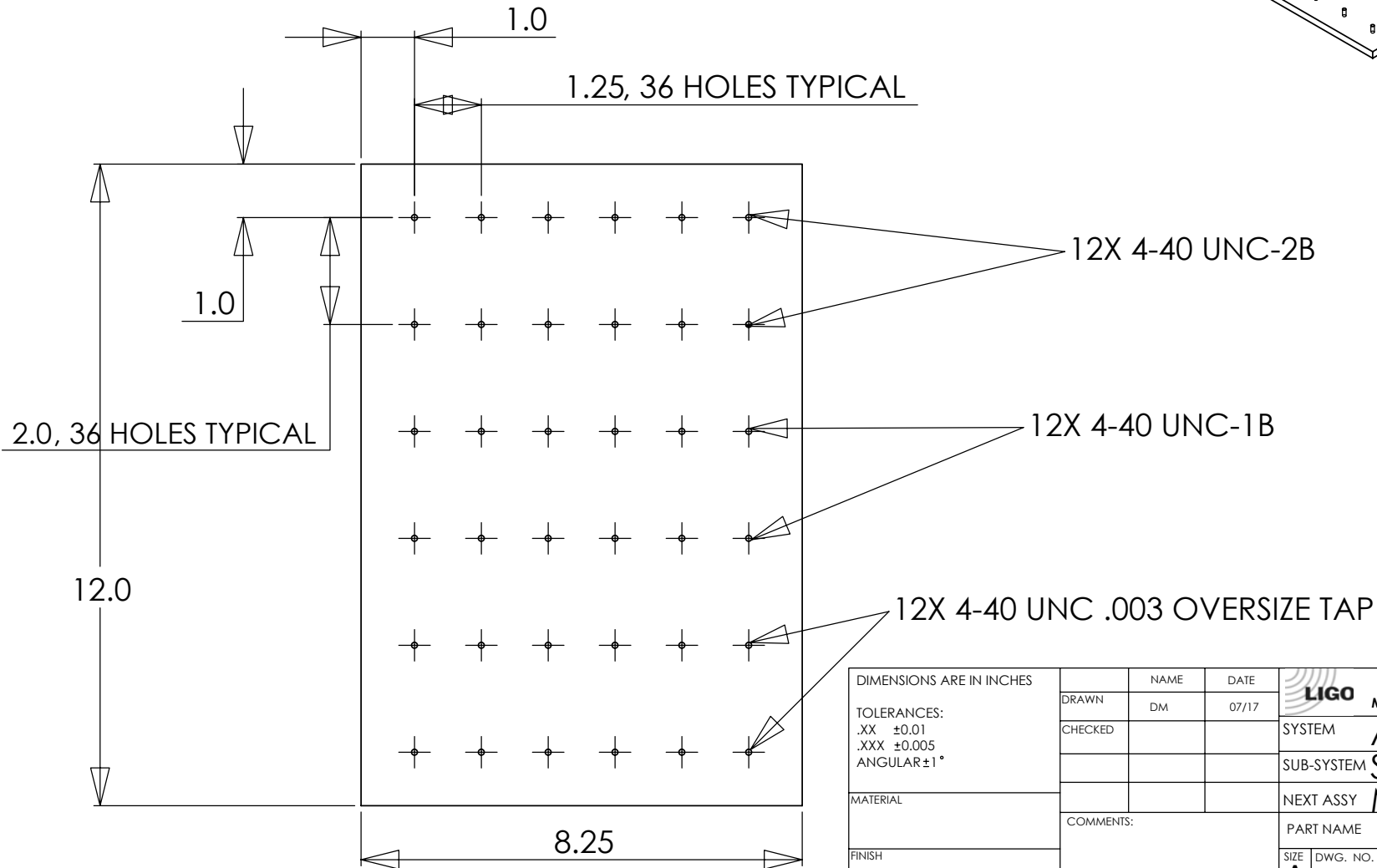
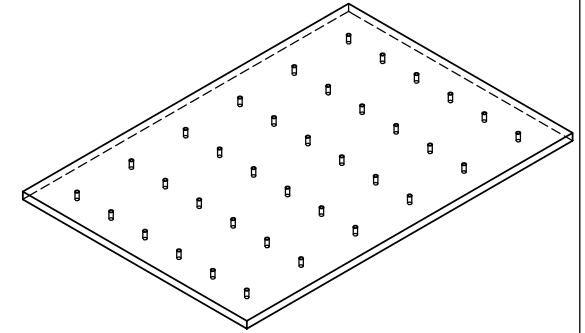
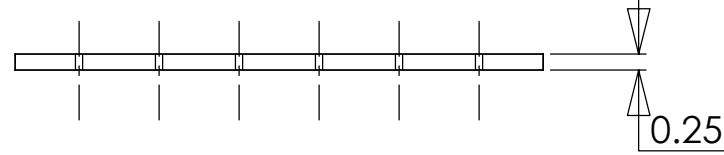


DIMENSIONS ARE IN INCHES		NAME	DATE	CALIFORNIA INSTITUTE OF TECHNOLOGY MASSACHUSETTS INSTITUTE OF TECHNOLOGY
TOLERANCES: .XX ±0.01 .XXX ±0.005 ANGULAR ±1°		DM	07/17	
MATERIAL	FINISH	COMMENTS:		SYSTEM ADVANCED LIGO
				SUB-SYSTEM SUS
				NEXT ASSY MC
				PART NAME COLD-WELDING PLATE 1/4
		SIZE A	DWG. NO. D02083-00-D	REV.
		SCALE: NTS		SHEET 1 OF 1

NOTES: (UNLESS OTHERWISE SPECIFIED)

1. DIMENSIONS IN INCHES
2. REMOVE ALL SHARP EDGES, R.02 MIN
3. ALL MACHINING FLUIDS SHALL BE WATER SOLUBLE AND FREE OF SULFUR, CHLORINE AND SILICONE, SUCH AS CINCINNATI MILACRON'S CIMTECH 410 (STAINLESS STEEL)
4. QUANTITY 2: ONE EACH OF MATERIALS ALUMINUM AND STAINLESS STEEL 300

REV.	DATE	DCN #	DRAWING TREE #

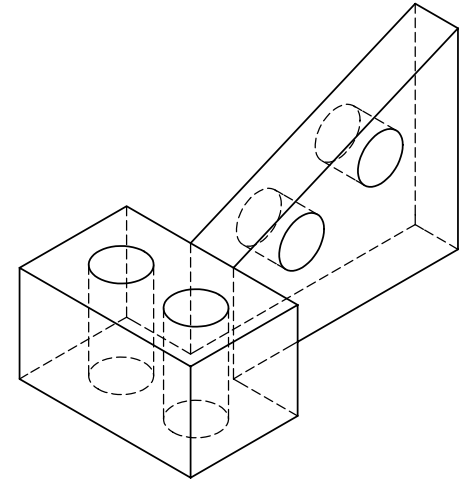
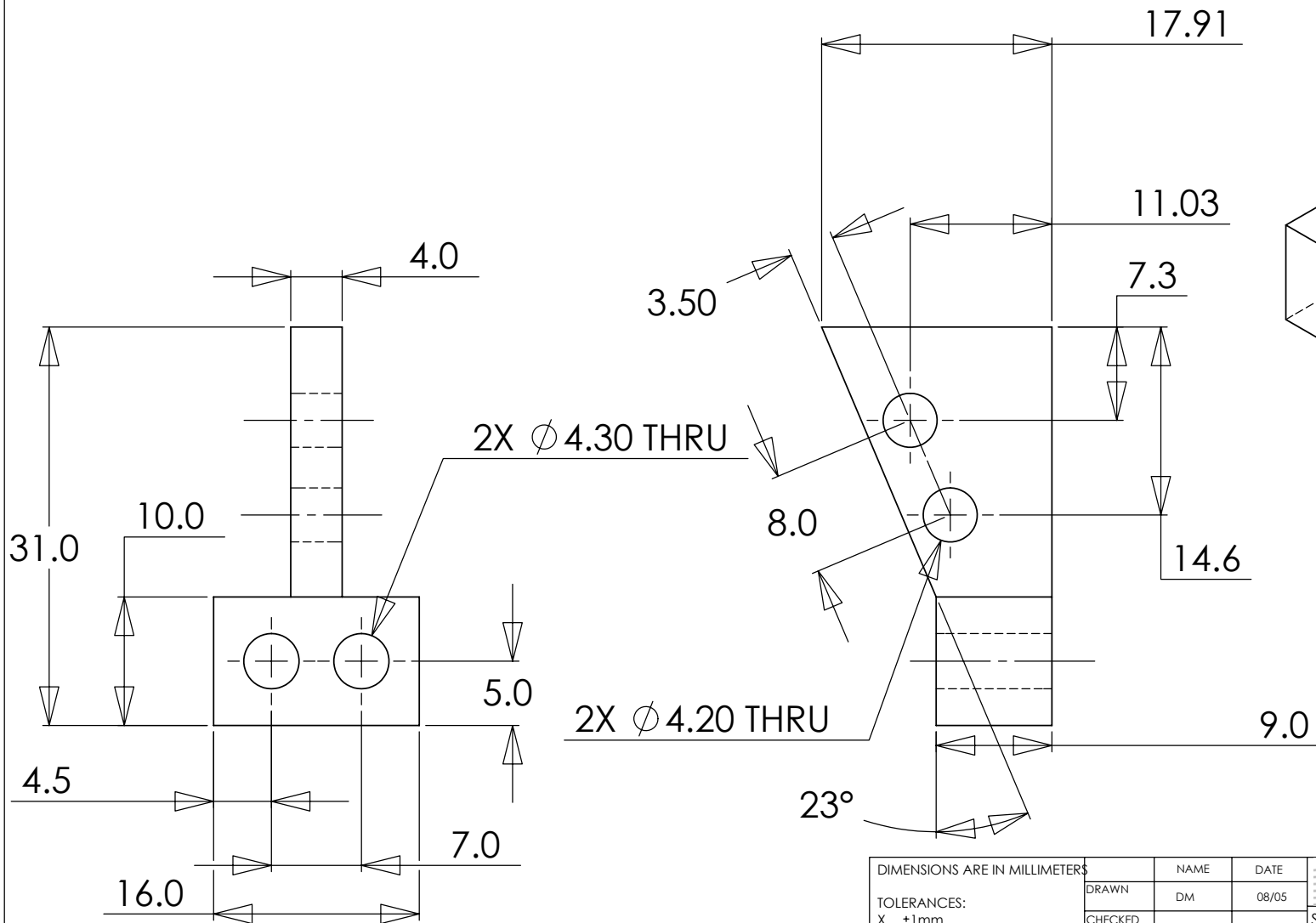



DIMENSIONS ARE IN INCHES		NAME	DATE	CALIFORNIA INSTITUTE OF TECHNOLOGY MASSACHUSETTS INSTITUTE OF TECHNOLOGY
TOLERANCES: .XX ±0.01 .XXX ±0.005 ANGULAR ±1°		DM	07/17	
MATERIAL		CHECKED		SYSTEM ADVANCED LIGO
FINISH		COMMENTS:		SUB-SYSTEM SUS
				NEXT ASSY MC
				PART NAME COLD-WELDING PLATE 4-40
		SIZE A	DWG. NO. D020384-00-D	REV.
		SCALE: NTS		SHEET 1 OF 1

NOTES: (UNLESS OTHERWISE SPECIFIED)

1. DIMENSIONS IN MILLIMETERS
2. REMOVE ALL SHARP EDGES
3. ALL MACHINING FLUIDS SHALL BE WATER SOLUBLE AND FREE OF SULFUR, CHLORINE AND SILICONE, SUCH AS CINCINNATI MILACRON'S CIMTECH 410 (STAINLESS STEEL)

REV.	DATE	DCN #	DRAWING TREE #



DIMENSIONS ARE IN MILLIMETERS		NAME	DATE	 CALIFORNIA INSTITUTE OF TECHNOLOGY MASSACHUSETTS INSTITUTE OF TECHNOLOGY
TOLERANCES: X. ±1mm X.X ±0.1mm X.XX ±0.05mm ANGULAR ±1°		DM	08/05	
MATERIAL	STAINLESS STEEL 300	CHECKED		SYSTEM ADVANCED LIGO
FINISH				SUB-SYSTEM SUS
				NEXT ASSY MC
		COMMENTS:		PART NAME BLADEWIRECLAMP STRAIGHT
		SCALE: NTS		SIZE A DWG. NO. D020429-00-D REV.
				SHEET 1 OF 1

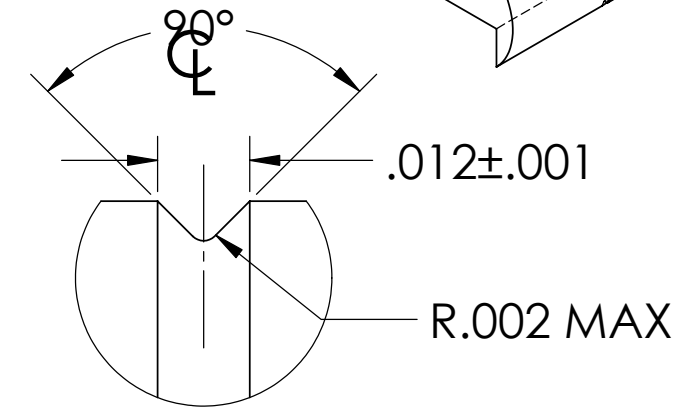
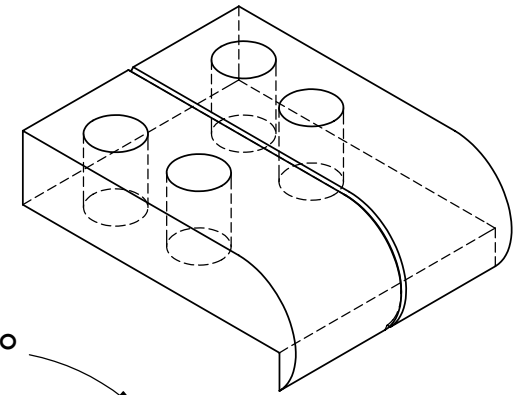
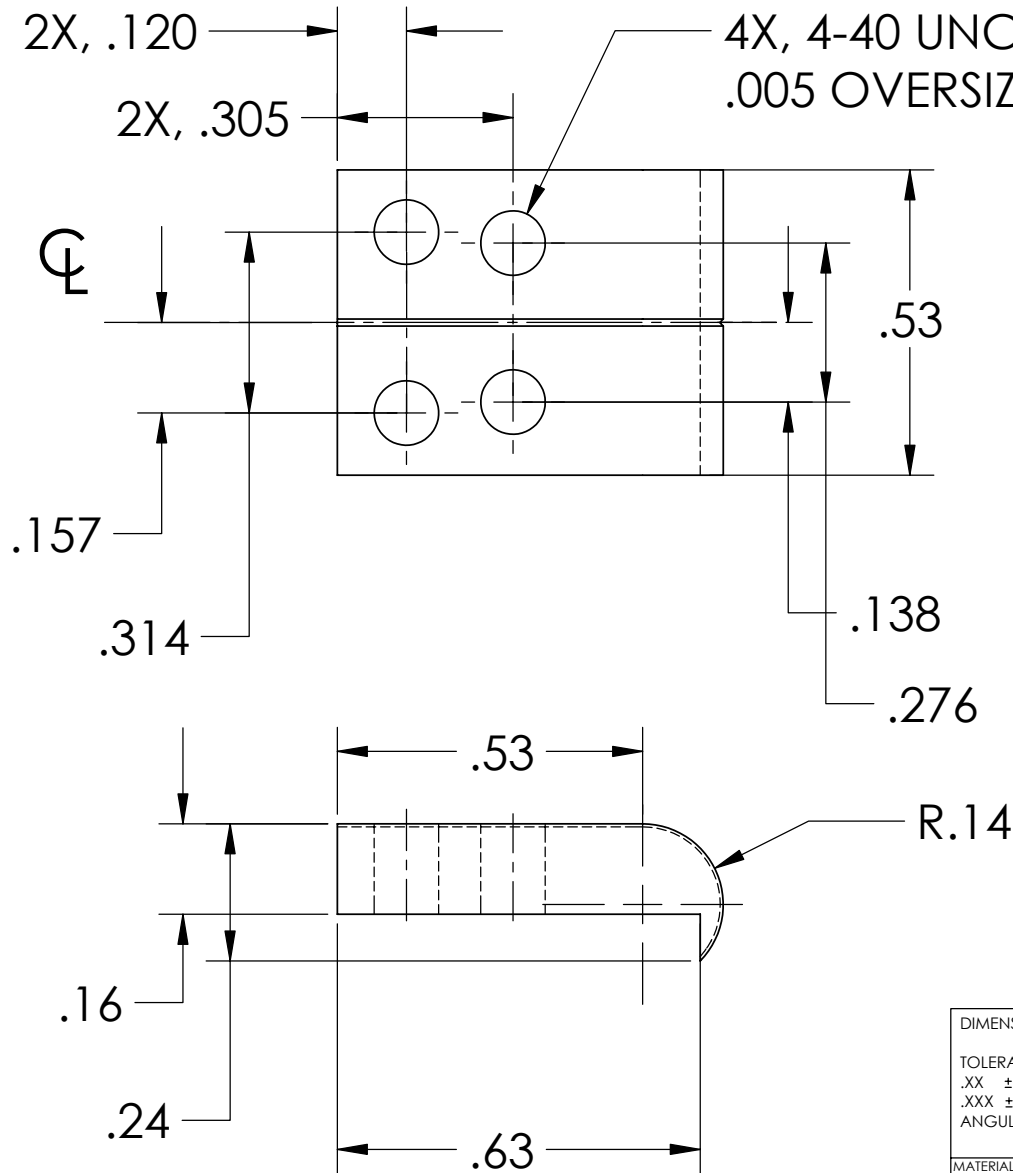
NOTES: (UNLESS OTHERWISE SPECIFIED)

1. DIMENSIONS IN INCHES

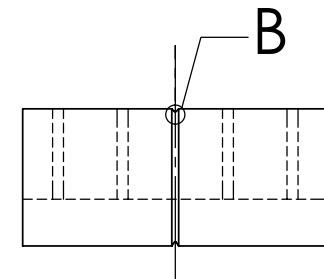
2. REMOVE ALL SHARP EDGES, R.02 MIN


3. ALL MACHINING FLUIDS SHALL BE WATER SOLUBLE AND FREE OF SULFUR, CHLORINE AND SILICONE, SUCH AS CINCINNATI MILACRON'S CIMTECH 410 (STAINLESS STEEL)

REV.	DATE	DCN #	DRAWING TREE #



DETAIL B
SCALE 40 : 1



DIMENSIONS ARE IN INCHES		NAME	DATE	 CALIFORNIA INSTITUTE OF TECHNOLOGY MASSACHUSETTS INSTITUTE OF TECHNOLOGY
TOLERANCES: .XX ±0.01 .XXX ±0.005 ANGULAR ±1°		DESIGN	D. MASON 08/02	
MATERIAL		DRAWN	CIT 08/02	SYSTEM ADVANCED LIGO
300 SERIES STAINLESS		CHECKED		SUB-SYSTEM SUS
FINISH		COMMENTS:		NEXT ASSY MC: UPPER MASS
				PART NAME ROUNDED UPPER BLADE CLAMP
		SIZE	DWG. NO.	REV.
		A	D020431	00
		SCALE: NTS		SHEET 1 OF 1